

# CONSTRUCTION OF A MEAN SQUARE ERROR ADAPTIVE EULER–MARUYAMA METHOD WITH APPLICATIONS IN MULTILEVEL MONTE CARLO

HÅKON HOEL<sup>†,‡</sup>, JUHO HÄPPÖLÄ<sup>†</sup>, AND RAÚL TEMPONE<sup>†</sup>

ABSTRACT. A formal mean square error expansion (MSE) is derived for Euler–Maruyama numerical solutions of stochastic differential equations (SDE). The error expansion is used to construct a pathwise *a posteriori* adaptive time stepping Euler–Maruyama method for numerical solutions of SDE, and the resulting method is incorporated into a multilevel Monte Carlo (MLMC) method for weak approximations of SDE. This gives an efficient MSE adaptive MLMC method for handling a number of low-regularity approximation problems. In low-regularity numerical example problems, the developed adaptive MLMC method is shown to outperform the uniform time stepping MLMC method by orders of magnitude, producing output whose error with high probability is bounded by  $\text{TOL} > 0$  at the near-optimal cost rate  $\mathcal{O}(\text{TOL}^{-2} \log(\text{TOL})^4)$ .

## CONTENTS

|  |    |
|--|----|
| 1. Introduction  | 1  |
| 1.1. Monte Carlo methods and the Euler–Maruyama scheme.          | 2  |
| 1.2. Uniform and adaptive time stepping MLMC                     | 3  |
| 2. Derivation of the MSE <i>a posteriori</i> adaptive method     | 6  |
| 2.1. The error expansion   | 6  |
| 2.2. The adaptive algorithm                                      | 7  |
| 2.3. Numerical examples  | 10 |
| 3. Extension of the adaptive algorithm to the multilevel setting | 12 |
| 3.1. Notation and objective                                      | 12 |
| 3.2. Error control   | 13 |
| 3.3. MLMC pseudocode   | 15 |
| 4. Numerical examples for the MLMC methods                       | 16 |
| 5. Conclusion  | 22 |
| Appendix A. Proofs   | 25 |
| A.1. Error expansion for the MSE in 1D                           | 25 |
| A.2. Error expansion for the MSE in multi-dimensions             | 29 |
| Appendix B. A uniform time step MLMC algorithm                   | 30 |
| References   | 31 |

## 1. INTRODUCTION

We consider the Itô stochastic differential equation (SDE)

$$\begin{aligned} dX_t &= a(t, X_t)dt + b(t, X_t)dW_t, & t \in (0, T), \\ X_0 &= x_0, \end{aligned} \tag{1}$$

---

2010 *Mathematics Subject Classification.* Primary 65C20; Secondary 65C05.

*Key words and phrases.* Adaptive time stepping, stochastic differential equations, multilevel Monte Carlo.

<sup>†</sup> Division of Mathematics, King Abdullah University of Science and Technology, Thuwal 23955-6900, Kingdom of Saudi Arabia (juho.happloa@kaust.edu.sa, raul.tempone@kaust.edu.sa).

<sup>‡</sup> Department of Mathematics, University of Oslo, P.O. Box1053, Blindern, NO-0316 Oslo, Norway (Corresponding author: haakonah@math.uio.no).

where  $X_t : [0, T] \rightarrow \mathbb{R}^d$  is a stochastic process with randomness generated by a  $k$ -dimensional Wiener process with independent components  $W_t(\omega)$ , and  $a : [0, T] \times \mathbb{R}^d \rightarrow \mathbb{R}^d$  and  $b : [0, T] \times \mathbb{R}^d \rightarrow \mathbb{R}^{d \times k}$  are the drift and diffusion coefficients, respectively. The contributions of this paper are twofold. First, an a posteriori adaptive time stepping algorithm for computing numerical realizations of SDE using the Euler–Maruyama method is developed. And second, for a given observable  $g : \mathbb{R}^d \rightarrow \mathbb{R}$ , we construct a mean square error (MSE) adaptive time stepping multilevel Monte Carlo (MLMC) algorithm for approximating the expected value  $\mathbb{E}[g(X_T)]$  under the following constraint

$$\mathbb{P}(|\mathbb{E}[g(X_T)] - \mathcal{A}| \leq \text{TOL}) \geq 1 - \delta. \quad (2)$$

Here,  $\mathcal{A}$  denotes the algorithm’s approximation of  $\mathbb{E}[g(X_T)]$  (examples of which are given in equations (3) and (7)) and  $\text{TOL}, \delta > 0$  are accuracy and confidence constraints, respectively. SDE models are frequently applied in mathematical finance [27, 26, 11], where an observable may for example represent the payoff of an option. SDE are also used to model the dynamics of multiscale physical, chemical or biochemical systems [10, 23, 28, 30], where, for instance, concentrations, temperature and energy may be sought observables.

**1.1. Monte Carlo methods and the Euler–Maruyama scheme.** Monte Carlo methods provide a robust and typically non-intrusive way to compute weak approximations of SDE. The convergence rate for MC methods does not depend on the dimension of the problem, and for that reason, MC is particularly effective on multi-dimensional problems. In its simplest form, MC approximations consist of the following two steps:

(A.1) Compute  $M$  numerical realizations  $\bar{X}_T(\omega_i)$  of the SDE (1).

(A.2) Approximate  $\mathbb{E}[g(X_T)]$  by the sample average

$$\mathcal{A} := \sum_{i=1}^M \frac{g(\bar{X}_T(\omega_i))}{M}. \quad (3)$$

As for ordinary differential equations, the theory for numerical integrators of different orders for scalar SDE is vast, and, provided sufficient regularity, higher order integrators generally yield higher convergence rates, cf. [19]. For MC methods it is straightforward to derive that the goal (2) is fulfilled at the computational cost  $\mathcal{O}(\text{TOL}^{-2-1/\alpha})$ , where  $\alpha \geq 0$  denotes the weak convergence rate of the numerical method, as defined in equation (5).

As numerical solver, we will in this paper only consider the Euler–Maruyama scheme

$$\begin{aligned} \bar{X}_{n+1} &= a(t_n, \bar{X}_n) \Delta t_n + b(t_n, \bar{X}_n) \Delta W_n, \\ \bar{X}_0 &= x_0, \end{aligned} \quad (4)$$

using time steps  $\Delta t_n = t_{n+1} - t_n$  and Wiener increments  $\Delta W_n = W_{t_{n+1}} - W_{t_n} \sim N(0, \Delta t_n)$ . The Euler–Maruyama scheme, which may be considered the SDE-equivalent of the forward Euler method for ODE, has, under sufficient regularity, first order weak convergence rate

$$|\mathbb{E}[g(X_T) - g(\bar{X}_T)]| = \mathcal{O}\left(\max_n \Delta t_n\right), \quad (5)$$

and also first order MSE convergence rate

$$\mathbb{E}\left[(g(X_T) - g(\bar{X}_T))^2\right] = \mathcal{O}\left(\max_n \Delta t_n\right), \quad (6)$$

cf. [19]. For multi-dimensional SDE problems, higher order schemes are generally less applicable, as either the diffusion coefficient matrix has to fulfill a rigid commutativity condition, or Levy areas, required in the higher order numerical schemes, has to be accurately approximated in order to achieve better convergence rates than those obtained with the Euler–Maruyama method, cf. [19].

**1.2. Uniform and adaptive time stepping MLMC.** MLMC is a class of MC methods that uses a hierarchy of subtly correlated and increasingly refined realization ensembles to reduce the variance of the sample estimator. In comparison to single-level MC, MLMC may yield orders of magnitude reductions in the computational cost of moment approximations. MLMC was first introduced by Heinrich [12, 13] for approximating integrals that depend on random parameters. For applications in SDE problems, Kebaier [18] introduced a two level MC method and proved its potential efficiency gains over single level MC. Giles [8] thereafter developed an MLMC method for SDE, proving even higher potential efficiency gains. Presently, MLMC is a vibrant research topic for which the list of contributions grows rapidly, e.g., [9, 3, 4, 32, 24, 21], and references therein.

1.2.1. *MLMC notation.* We define the multilevel estimator by

$$\mathcal{A}_{MLC} := \sum_{\ell=0}^L \sum_{i=1}^{M_\ell} \frac{\Delta_\ell g(\omega_{i,\ell})}{M_\ell}, \tag{7}$$

where

$$\Delta_\ell g(\omega_{i,\ell})(\omega) := \begin{cases} g\left(\overline{X}_T^{\{0\}}(\omega)\right), & \text{if } \ell = 0, \\ g\left(\overline{X}_T^{\{\ell\}}(\omega)\right) - g\left(\overline{X}_T^{\{\ell-1\}}(\omega)\right), & \text{otherwise,} \end{cases}$$

$L$  denotes the number of levels,  $M_\ell$  the number of sample realizations on the  $\ell$ -th level, and the realization pair  $\overline{X}_T^{\{\ell\}}(\omega_{i,\ell})$  and  $\overline{X}_T^{\{\ell-1\}}(\omega_{i,\ell})$  are generated by the Euler–Maruyama method (4) using the *same* Wiener path  $W_t(\omega_{i,\ell})$  sampled on the respective meshes  $\Delta t^{\{\ell\}}$  and  $\Delta t^{\{\ell-1\}}$ , cf. Figure 1. For consistency, we also introduce the notation  $W^{\{\ell\}}(\omega)$  for the Wiener path restricted to the mesh  $\Delta t^{\{\ell\}}(\omega)$ .

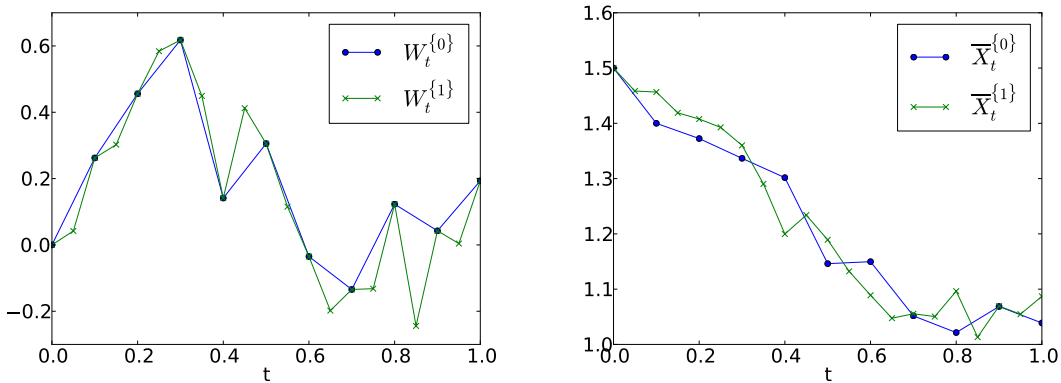


FIGURE 1. (Left) A sample Wiener path  $W_t$  generated on the coarse mesh  $\Delta t^{\{0\}}$  with uniform step size 1/10 (blue line). The path is thereafter Brownian bridge interpolated onto a finer mesh  $\Delta t^{\{1\}}$ , which has uniform step size 1/20 (green line). (Right) Euler–Maruyama numerical solutions of the Ornstein-Uhlenbeck SDE problem  $dX_t = 2(1 - X_t)dt + 0.2dW_t$ , with initial condition  $X_0 = 3/2$ , are computed on the meshes  $\Delta t^{\{0\}}$  (blue line) and  $\Delta t^{\{1\}}$  (green line) using Wiener increments from the respective path resolutions.

1.2.2. *Uniform time step MLMC.* For the uniform time step MLMC introduced in [8], the respective SDE realizations  $\{\overline{X}_T^{\{\ell\}}\}_\ell$  are constructed on a hierarchy of uniform meshes with geometrically decaying step size  $\Delta t^{\{\ell\}} = T/N_\ell$ , and  $N_\ell = m^\ell N_0$  with  $m \in \mathbb{N} \setminus \{1\}$  and a preset initial number of samples  $N_0 \in \mathbb{N} \cap \mathcal{O}(1)$ . For simplicity, we will in this paper consider the uniform time step MLMC method with  $m = 2$ .

1.2.3. *MLMC error and computational complexity.* By construction, the multilevel estimator is telescoping, i.e.,  $\mathbb{E}[\mathcal{A}_{\mathcal{M}\mathcal{L}}] = \mathbb{E}\left[g\left(\overline{X}_T^{\{L\}}\right)\right]$ . Using this property, we may conveniently bound the multilevel approximation error

$$|\mathbb{E}[g(X_T)] - \mathcal{A}_{\mathcal{M}\mathcal{L}}| \leq \underbrace{\left|\mathbb{E}\left[g(X_T) - g\left(\overline{X}_T^{\{L\}}\right)\right]\right|}_{=:\epsilon_T} + \underbrace{\left|\mathbb{E}\left[g\left(\overline{X}_T^{\{L\}}\right) - \mathcal{A}_{\mathcal{M}\mathcal{L}}\right]\right|}_{=:\epsilon_S}.$$

The approximation goal (2) then is reached by ensuring that the sum of the *bias*  $\epsilon_T$  and the *statistical error*  $\epsilon_S$  is bounded from above by TOL, e.g., by the constraints  $\mathcal{E}_T \leq \text{TOL}/2$  and  $\mathcal{E}_S \leq \text{TOL}/2$ , see Section 3.2 for more details on the MLMC error control. For the MSE error goal

$$\mathbb{E}\left[\left(\mathbb{E}[g(X_T)] - \mathcal{A}_{\mathcal{M}\mathcal{L}}\right)^2\right] \leq \text{TOL}^2$$

the following theorem states the optimal computational cost for MLMC:

**Theorem 1.1** (Cliffe et al. [4]). *Suppose there are constants  $\alpha, \beta, \gamma$  such that  $\alpha \geq \frac{\min(\beta, \gamma)}{2}$  and*

- (i)  $\left|\mathbb{E}\left[g\left(\overline{X}_T^{\{\ell\}}\right) - g(X_T)\right]\right| = \mathcal{O}(N_\ell^{-\alpha})$ ,
- (ii)  $\text{Var}(\Delta_\ell g) = \mathcal{O}(N_\ell^{-\beta})$ ,
- (iii)  $\text{Cost}(\Delta_\ell g(\omega)) = \mathcal{O}(N_\ell^\gamma)$ .

*Then, for any  $\text{TOL} < e^{-1}$  there exists an  $L$  and a sequence  $\{M_\ell\}_{\ell=0}^L$  such that*

$$\mathbb{E}\left[\left(\mathcal{A}_{\mathcal{M}\mathcal{L}} - \mathbb{E}[g(X_T)]\right)^2\right] \leq \text{TOL}^2, \quad (8)$$

and

$$\text{Cost}(\mathcal{A}_{\mathcal{M}\mathcal{L}}) = \begin{cases} \mathcal{O}(\text{TOL}^{-2}), & \text{if } \beta > \gamma, \\ \mathcal{O}(\text{TOL}^{-2} \log(\text{TOL})^2), & \text{if } \beta = \gamma, \\ \mathcal{O}(\text{TOL}^{-2 + \frac{\beta - \gamma}{\alpha}}), & \text{if } \beta < \gamma. \end{cases}$$

In comparison, the computational cost of achieving the goal (8) with single-level MC is  $\mathcal{O}(\text{TOL}^{-2 - \gamma/\alpha})$ . Theorem 1.1 thus shows that for any problem with  $\beta > 0$ , MLMC will asymptotically be more efficient than single-level MC. Furthermore, the performance gain of MLMC over MC is particularly apparent in settings where  $\beta \geq \gamma$ . The latter property is linked to the contributions of this paper, as for some low-regularity SDE problems, e.g., Example 4.2 and [33, 1], uniform time step Euler–Maruyama results in convergence rates for which  $\beta < \gamma$ , whereas the adaptive Euler–Maruyama can preserve rates such that  $\beta \geq \gamma$ . In other words, for low-regularity problems, adaptive time stepping MLMC can be orders of magnitude less costly than uniform time stepping MLMC.

*Remark 1.1.* Similar accuracy vs. complexity results to Theorem 1.1, requiring slightly stronger moment bounds, have also been derived for the approximation goal (2) in the asymptotic setting when  $\text{TOL} \downarrow 0$ , cf. [14, 5].

1.2.4. *MSE a posteriori adaptive time stepping.* Adaptive time stepping algorithms seek to fulfill one of two equivalent goals [2]:

- (B.1) Provided a computational budget  $N$ , determine the possibly non-uniform mesh which minimizes the error  $\|g(X_T) - g(\overline{X}_T)\|$ .
- (B.2) Provided an error constraint  $\|g(X_T) - g(\overline{X}_T)\| \leq \text{TOL}$ , determine the possibly non-uniform mesh which achieves the constraint at the minimum computational cost.

Evidently, the refinement criterion of an adaptive algorithm depends on the error one seeks to minimize. In this paper, we consider the adaptivity goal (B.1) with the error measured in terms of the MSE. This error measure is suitable for MLMC methods as it often will lead to improved convergence rate  $\beta$  (since  $\text{Var}(\Delta_\ell g) \leq \mathbb{E}[\Delta_\ell g^2]$ ), which by Theorem 1.1 may reduce the

computational cost of MLMC. In Theorem 2.1, we derive the following error expansion for the MSE of Euler–Maruyama numerical solutions of the SDE (1)

$$\mathbb{E}\left[\left(g(X_T) - g(\bar{X}_T)\right)^2\right] = \mathbb{E}\left[\sum_{n=0}^{N-1} \bar{\rho}_n \Delta t_n^2 + o(\Delta t_n^2)\right], \tag{9}$$

where the error density  $\bar{\rho}_n$  is a function of the local error and sensitivities from the dual solution of the SDE problem, as defined in (16). The error expansion (9) is an *a posteriori* error estimate for the MSE, and in our adaptive method the mesh is refined by equilibration of the expansion’s *error indicators*

$$\bar{r}_n := \bar{\rho}_n \Delta t_n^2, \quad \text{for } n = 0, 1, \dots, N - 1. \tag{10}$$

1.2.5. *An MSE adaptive MLMC method.* Using the described MSE adaptive algorithm, we construct an MSE adaptive MLMC method in Section 3. The MLMC method generates SDE realizations  $\{\bar{X}_T^{(\ell)}\}_\ell$  on a hierarchy of *pathwise* adaptively refined meshes  $\{\Delta t^{(\ell)}\}_\ell$ . The meshes are nested, i.e., for all realizations  $\omega \in \Omega$ ,

$$\Delta t^{(0)}(\omega) \subset \Delta t^{(1)}(\omega) \subset \dots \Delta t^{(\ell)}(\omega) \subset \dots,$$

and have the constraint that  $\Delta t^{(\ell)}$  contains less than  $2N_\ell = 2^{\ell+2}N_{-1}$  time steps, where  $N_{-1} = \mathbb{N} \cap \mathcal{O}(1)$  is a preset pre-initial number of time steps. (Compare to the mesh hierarchy setup for the uniform time step MLMC method in Section 1.2.2.)

The potential efficiency gain of adaptive MLMC is experimentally illustrated in the drift blow-up problem

$$dX_t = \frac{rX_t}{|t - \xi|^p} dt + \sigma X_t dW_t, \quad X_0 = 1,$$

which we study in Example 4.2 for the three different singularity exponents  $p = 1/2, 2/3$  and  $3/4$ , with a pathwise, random singularity point  $\xi \sim U(1/4, 3/4)$ , an observable  $g(x) = x$ , and a final time  $T = 1$ . For the given singularity exponents, we observe experimental convergence rates  $\alpha = (1 - p)$  and  $\beta = 2(1 - p)$  for uniform time step Euler–Maruyama, while for adaptive time step Euler–Maruyama we observe  $\alpha \approx 1$  and  $\beta \approx 1$ . Then, as predicted by Theorem 1.1, we also observe an order of magnitude difference in computational cost between the two methods, cf. Table 1.

TABLE 1. Observed computational cost – disregarding  $\log(\text{TOL})$  multiplicative factors of finite order – for the drift blow-up study in Example 4.2

| Singularity exponent $p$ | Observed computational cost |                   |
|--------------------------|-----------------------------|-------------------|
|                          | Adaptive MLMC               | Uniform MLMC      |
| 1/2                      | $\text{TOL}^{-2}$           | $\text{TOL}^{-2}$ |
| 2/3                      | $\text{TOL}^{-2}$           | $\text{TOL}^{-3}$ |
| 3/4                      | $\text{TOL}^{-2}$           | $\text{TOL}^{-4}$ |

1.2.6. *Earlier works on adaptivity for SDE.* Gaines’ and Lyons’ paper [7] is one of the early and substantial works on adaptive methods for SDE. They present a method that seeks to minimize the *pathwise* error of the mean and variation of the local error conditioned on the  $\sigma$ -algebra generated by  $\{W_{t_n}\}_{n=1}^N$  (i.e., the values at which the Wiener path has been evaluated in order to numerically integrate the SDE realization). The method may be used in combination with different numerical integration methods, and an approach to approximations of potentially needed Levy areas is proposed, facilitated by a binary tree representation of the Wiener path realization at its evaluation points. As for a *a posteriori* adaptive methods, Gaines’ and Lyons’ method’s error indicators are given by products of local errors and weight terms, but, unlike for a *a posteriori* methods, the weight terms are computed from *a priori* estimates.

A *posteriori* weak error based adaptivity for the Euler–Maruyama method with numerically computable error indicator terms was introduced by Szepessy et al. [29]. Their development of weak error adaptivity took inspiration from Talay and Tubaro’s seminal work [31], where an error expansion for the weak error was derived for the Euler–Maruyama method when using uniform time steps. In [14], Szepessy et al.’s weak error adaptive method was used in the construction of a weak error adaptive MLMC method. To the best of our knowledge, the present work is the first on MSE *a posteriori* adaptive methods for SDE both in the MC- and MLMC setting.

Among other adaptive methods for SDE, many have refinement criteria based only or primarily on estimates of the local error. See for example [15], where the step-size depends on the size of the diffusion coefficient for a MSE Euler–Maruyama adaptive method; the work [20], where the step-size is controlled by the size of the drift coefficient variation in the constructed Euler–Maruyama adaptive method that preserves the long term ergodic behavior of the true solution for many SDE problems; and [17], where a local error based adaptive Milstein method is developed for solving multi-dimensional chemical Langevin equations.

**Organization.** The rest of the paper is organized as follows. The theory, framework and numerical examples for the MSE adaptive method is presented in Section 2. In Section 3, we develop the framework for the MSE adaptive MLMC method and present implementational details in algorithms with pseudocode. In Section 4, we compare the performance of the MSE adaptive- and uniform MLMC methods in a couple of numerical examples, one of which is a low-regularity SDE problem. Thereafter, we wrap up with conclusions.

## 2. DERIVATION OF THE MSE *a posteriori* ADAPTIVE METHOD

In this section, we construct an MSE *a posteriori* adaptive method for SDE whose realizations are numerically integrated by the Euler–Maruyama method (4). Our goal is a method for solving the SDE problem (1) that for a fixed number of intervals  $N$ , determines the time stepping  $\Delta t_0, \Delta t_1, \dots, \Delta t_{N-1}$  so that the MSE  $\mathbb{E} \left[ (g(\bar{X}_T) - g(X_T))^2 \right]$  is minimized. That is,

$$\mathbb{E} \left[ (g(\bar{X}_T) - g(X_T))^2 \right] \rightarrow \min!, \quad N \text{ given} \quad (11)$$

The derivation of our adaptive method consists of two steps. First, an error expansion for the MSE is presented in Theorem 2.1. Based on the error expansion, we thereafter construct a mesh refinement algorithm. At the end of the section, we apply the adaptive algorithm to a few example problems.

**2.1. The error expansion.** Let us now present a leading order error expansion for the MSE (11) of the SDE problem (1) in the 1D setting, i.e., when  $X_t \in \mathbb{R}$  and the drift and diffusion coefficients respectively are of the form  $a : \mathbb{R} \times [0, T] \rightarrow \mathbb{R}$  and  $b : \mathbb{R} \times [0, T] \rightarrow \mathbb{R}$ . An extension of the MSE error expansion to multi-dimensions is given in Appendix A.2. For stating the error expansion result, the following notation is needed:  $X_T^{x,t}$  denotes a solution of the SDE (1) conditioned that  $X_t = x$ ,  $X_T$  is shorthand for  $X_T^{x_0,0}$ , and for a given observable  $g$ , the payoff-of-flow map function is defined by  $\varphi(x, t) = g(X_T^{x,t})$ .

**Theorem 2.1** (1D MSE leading order error expansion). *Let  $\bar{\varphi}_{x,n} := \frac{\partial}{\partial X_n} g(\bar{X}_T)$  and assume all needed moments of derivatives of  $a(X_t, t)$ ,  $b(X_t, t)$ ,  $g(X_T)$  and  $\varphi(X_t, t)$  are bounded for all times  $t \in [0, T]$ , that all needed moments of derivatives of  $a(\bar{X}_n, t_n)$ ,  $b(\bar{X}_n, t_n)$ ,  $g(\bar{X}_T)$  and  $\bar{\varphi}_{x,n}$  are bounded at all mesh points  $t_0, t_1, \dots, t_N$  and that  $\max_n \Delta t_n = o(1)$ . Then*

$$\mathbb{E} \left[ (g(X_T) - g(\bar{X}_T))^2 \right] = \mathbb{E} \left[ \sum_{n=0}^{N-1} \bar{\varphi}_{x,n}^2 \frac{(b_x b)^2}{2} (\bar{X}_n, t_n) \Delta t_n^2 + o(\Delta t_n^2) \right]. \quad (12)$$

*Remark 2.1.* For low-regularity SDE problems the actual leading order term of the MSE (12) may contain other or additional terms in the error density. See Example 4.2 for a problem where *ad hoc* additional terms are added to the error density.

*Remark 2.2.* Stricter regularity conditions can be provided in Theorem 2.1. For the applications on low-regularity SDE problems, however, sharp regularity conditions are not that interesting, as they will typically not be fulfilled. In our adaptive method, the error expansion (12) is interpreted in a formal sense and only used to facilitate the construction of a mesh refinement criterion.

2.1.1. *Numerical approximation of the first variation.* Formally,  $\varphi_x(x, t) = \frac{\partial}{\partial x} g(X_T^{x,t})$  solves the backward SDE

$$\begin{aligned} -d\varphi_x(X_s^{x,t}, s) &= (a_x(X_s^{x,t}, s)ds + b_x(X_s^{x,t}, s)dW_s) \varphi_x(X_s^{x,t}, s), \quad t < s < T \\ \varphi_x(X_T^{x,t}, T) &= g'(X_T^{x,t}), \end{aligned} \quad (13)$$

cf. [29]. To obtain an all-terms-computable error expansion in Theorem 2.1 – which will be needed to construct an *a posteriori* adaptive method – the first variation

$$\varphi_x(x, t) = \frac{\partial}{\partial x} g(X_T(x, t))$$

has been replaced by the first variation of the Euler–Maruyama numerical solution,

$$\bar{\varphi}_{x,n} = \frac{\partial}{\partial \bar{X}_n} g(\bar{X}_T).$$

And  $\bar{\varphi}_{x,n}(\omega)$  is a solution to the backward scheme

$$\bar{\varphi}_{x,n} = c_x(\bar{X}_n, t_n) \bar{\varphi}_{x,n+1}, \quad n = N-1, N-2, \dots, 1, \quad (14)$$

with the initial condition  $\bar{\varphi}_{x,N} = g'(\bar{X}_T)$  and

$$c(\bar{X}_n, t_n) := \bar{X}_n + a(\bar{X}_n, t_n)\Delta t_n + b(\bar{X}_n, t_n)\Delta W_n. \quad (15)$$

This follows from the following recursive relation

$$\begin{aligned} \frac{\partial}{\partial \bar{X}_n} g(\bar{X}_T^{\bar{X}_n, t_n}) &= \frac{\partial}{\partial \bar{X}_{n+1}} g\left(\bar{X}_T^{\bar{X}_{n+1}, t_{n+1}}\right) \frac{\partial \bar{X}_{n+1}}{\partial \bar{X}_n} \\ &= \bar{\varphi}_{x,n+1} \cdot \frac{\partial(\bar{X}_n + a(\bar{X}_n, t_n)\Delta t_n + b(\bar{X}_n, t_n)\Delta W_n)}{\partial \bar{X}_n} \\ &= \bar{\varphi}_{x,n+1} \cdot (1 + a_x(\bar{X}_n, t_n)\Delta t_n + b_x(\bar{X}_n, t_n)\Delta W_n). \end{aligned}$$

**2.2. The adaptive algorithm.** Having derived computable expressions for all the terms in the error expansion, we next introduce the error density

$$\bar{\rho}_n := \bar{\varphi}_{x,n}^2 \frac{(b_x b)^2}{2}(\bar{X}_n, t_n), \quad n = 0, 1, \dots, N-1, \quad (16)$$

and, for representing the numerical solution's error contribution from the time interval  $(t_n, t_{n+1})$ , the error indicators

$$\bar{r}_n := \bar{\rho}_n \Delta t_n^2, \quad n = 0, 1, \dots, N-1. \quad (17)$$

The error expansion (12) may then be written

$$\mathbb{E} \left[ (g(X_T) - g(\bar{X}_T))^2 \right] = \mathbb{E} \left[ \sum_{n=0}^{N-1} \bar{r}_n + o(\Delta t_n^2) \right]. \quad (18)$$

The final goal of the adaptive algorithm is minimization of the leading order of the MSE  $\mathbb{E} \left[ \sum_{n=0}^{N-1} \bar{r}_n \right]$ , which (for each realization) is approached by minimization of the error expansion realization  $\sum_{n=0}^{N-1} \bar{r}_n(\omega)$ . An approximately optimal choice for the refinement procedure can be derived by introducing the Lagrangian

$$\mathcal{L}(\Delta t, \lambda) = \int_0^T \frac{1}{\Delta t(s)} ds + \lambda \left( \int_0^T \rho(s) \Delta t(s) ds - \text{TOL} \right), \quad (19)$$

for which we seek to minimize the number of time steps

$$N \approx \int_0^T \frac{1}{\Delta t(s)} ds$$

with the constraint that

$$\underbrace{\int_0^T \rho(s) \Delta t(s) ds}_{\approx \sum_{n=0}^{N-1} \bar{r}_n} \leq \text{TOL}. \quad (20)$$

Minimizing (19) yields

$$\Delta t_n = \sqrt{\frac{\text{TOL}}{N \rho(t_n)}} \quad \text{and} \quad \mathbb{E}[N] = \text{TOL}^{-1} \mathbb{E} \left[ \left( \int_0^T \sqrt{\rho(s)} ds \right)^2 \right]. \quad (21)$$

In comparison, we notice that for if using a uniform mesh, the cost becomes

$$\mathbb{E}[N_{\text{uniform}}] = \frac{T}{\text{TOL}} \mathbb{E} \left[ \int_0^T \rho(s) ds \right]. \quad (22)$$

It is easy to see from (21) and (22) that for many low-regularity problems, adaptive time stepping Euler–Maruyama fulfills the constraint (20) at the cost  $\mathcal{O}(\text{TOL}^{-1})$ , whereas uniform time stepping Euler–Maruyama will require a higher order cost to do it.

**2.2.1. Mesh refinement strategy.** The optimal time stepping (21) leads to equilibrated error indicators:

$$\bar{r}_n = \bar{\rho}_n \Delta t_n^2 = \frac{\text{TOL}}{N}, \quad n = 0, 1, \dots, N-1.$$

We propose a mesh refinement strategy which tries to mimic the equilibration of error indicators by iteratively identifying the largest error indicator and refining the corresponding time interval by halving.

To compute the error indicators prior to refinement, the algorithm first computes the numerical SDE solution  $\bar{X}_n$  and the corresponding first variation  $\bar{\varphi}_{x,n}$  (using equations (4) and (14) respectively) on the initial mesh  $\Delta t$ . Thereafter, the error indicators  $\bar{r}_n$  are computed by equation (17) and the mesh is refined a prescribed number of times  $N_{\text{refine}}$  as follows:

(C.1) Find the largest error indicator

$$n^* := \arg \max_n \bar{r}_n, \quad (23)$$

and refine the corresponding time step by halving

$$(t_{n^*}, t_{n^*+1}) \rightarrow \left( t_{n^*}, \underbrace{\frac{t_{n^*} + t_{n^*+1}}{2}}_{=t_{n^*+1}^{\text{new}}}, \underbrace{t_{n^*+1}}_{=t_{n^*+2}^{\text{new}}} \right). \quad (24)$$

(C.2) Update the values of the error indicators, either by recomputing the whole problem or locally by interpolation.

(C.3) Go to step (C.4) if  $N_{\text{refine}}$  mesh refinements have been made; otherwise, return to step (C.1).

(C.4) (Postconditioning) Do a last sweep over the mesh and refine by halving every time step that is strictly larger than  $\Delta t_{\text{max}}$ , where  $\Delta t_{\text{max}} = \mathcal{O}(N^{-\psi})$ ,  $\psi \in (0, 1]$  denotes the maximum allowed step size.

The postconditioning step (C.4) ensures that all time steps become infinitesimally small as the final number of time steps  $N \rightarrow \infty$ . Under classical smoothness assumptions and the assumption that the adaptive numerical solution is  $\mathcal{F}_t$ -adapted, where  $\mathcal{F}_t$  denotes the sigma-algebra  $\sigma(\{W_s\}_{0 \leq s \leq t})$ , the step (C.4) implies both weak convergence and MSE convergence for numerical solutions of the MSE adaptive Euler–Maruyama method (the  $\mathcal{F}_t$ -adaptedness assumption does however not hold in general). That is,

$$\lim_{N \rightarrow \infty} \max \left\{ \left| \mathbb{E}[g(X_T) - g(\bar{X}_T)] \right|, \mathbb{E} \left[ |g(X_T) - g(\bar{X}_T)|^2 \right] \right\} = 0.$$

2.2.2. *Wiener path refinements.* When a time step is refined, as described in (24), the Wiener path must be refined correspondingly. The value of the Wiener path at the midpoint between  $W_{t_n^*}$  and  $W_{t_{n^*+1}}$  can be generated by Brownian bridge interpolation

$$W_{n^*+1}^{new} = \frac{W_{n^*} + W_{n^*+1}}{2} + \xi \frac{\sqrt{\Delta t_{n^*}}}{2}, \quad (25)$$

where  $\xi \sim N(0,1)$ , cf. [25]. See Figure 1 for an illustration of Brownian bridge interpolation applied to numerical solutions of an Ornstein-Uhlenbeck SDE.

2.2.3. *Updating the error indicators.* After the refinement of an interval  $(t_{n^*}, t_{n^*+1})$  and its Wiener path, error indicators must also be updated before moving on to determine which interval is next in line for refinement. There are different ways of updating error indicators. One expensive but more accurate option is to recompute the error indicators completely by first solving the forward problem (4) and the backward problem (14). A less costly but also less accurate alternative, is to only update the error indicators locally at the refined time step by one forward and backward numerical solution step, respectively:

$$\begin{aligned} \bar{X}_{n^*+1}^{new} &= \bar{X}_{n^*} + a(\bar{X}_{n^*}, t_{n^*})\Delta t_{n^*}^{new} + b(\bar{X}_{n^*}, t_{n^*})\Delta W_{n^*}^{new}, \\ \bar{\varphi}_{x,n^*+1}^{new} &= c_x(\bar{X}_{n^*}^{new}, t_{n^*}^{new})\bar{\varphi}_{x,n^*+1}. \end{aligned} \quad (26)$$

And, thereafter compute the resulting error density  $\bar{\rho}_{n^*+1}^{new}$  by equation (16), and finally update the error locally by

$$\bar{r}_{n^*} = \bar{\rho}_{n^*} (\Delta t_{n^*}^{new})^2, \quad \bar{r}_{n^*+1} = \bar{\rho}_{n^*+1}^{new} (\Delta t_{n^*+1}^{new})^2. \quad (27)$$

As a compromise between cost and accuracy, we here propose the following mixed approach to updating error indicators post refinement: With  $N_{\text{refine}}$  denoting the prescribed number of refinement iterations of the input mesh, let all error indicators be completely recomputed every  $\tilde{N} = \mathcal{O}(\log(N_{\text{refine}}))$ -th iteration, whereas for the remaining  $N_{\text{refine}} - \tilde{N}$  iterations, only local updates of the error indicators are computed. Following this approach, the computational cost of refining a mesh holding  $N$  time steps into a mesh of  $2N$  time steps becomes  $\mathcal{O}(N \log(N)^2)$  (the asymptotically dominating cost is to sort the mesh's error indicators  $\mathcal{O}(\log(N))$  times). To anticipate the computational cost for the MSE adaptive MLMC method, this implies that the cost of generating an MSE adaptive realization pair is  $\text{Cost}(\Delta_{\ell g}) = \mathcal{O}(\ell^2 2^\ell)$ .

2.2.4. *Pseudocode.* The mesh refinement and the computation of error indicators are presented in Algorithms 1 and 2, respectively.

**Algorithm 1 meshRefinement**


---

**Input:** Mesh  $\Delta t$ , Wiener path  $W$ , number of refinements  $N_{\text{refine}}$ , maximum time step  $\Delta t_{\text{max}}$

**Output:** Refined mesh  $\Delta t$  and Wiener path  $W$ .

Set the number of re-computations of all error indicators to a number  $\tilde{N} = \mathcal{O}(\log(N_{\text{refine}}))$  and compute the refinement batch size  $\hat{N} = \lceil N_{\text{refine}}/\tilde{N} \rceil$ .

**for**  $i = 1$  **to**  $\tilde{N}$  **do**

Completely update the error density by calling  
 $[\bar{r}, \bar{X}, \bar{\varphi}_x, \bar{\rho}] = \text{computeErrorDensity}(\Delta t, W)$ .

**if**  $N_{\text{refine}} > 2\hat{N}$  **then**

Set the below for-loop limit to  $J = \hat{N}$ .

**else**

Set  $J = N_{\text{refine}}$ .

**end if**

**for**  $j = 1$  **to**  $J$  **do**

Locate the largest error indicator  $\bar{r}_{n^*}$  using equation (23).

Refine the interval  $(t_{n^*}, t_{n^*+1})$  by the halving (24), add a midpoint value  $W_{n^*+1}^{\text{new}}$  to the Wiener path by the Brownian bridge interpolation (25), and set  $N_{\text{refine}} = N_{\text{refine}} - 1$ .

Locally update the error indicators  $r_{n^*}^{\text{new}}$  and  $r_{n^*+1}^{\text{new}}$  by the steps (26) and (27).

**end for**

**end for**

Do a final sweep over the mesh and refine all time steps of the input mesh which are strictly larger than  $\Delta t_{\text{max}}$ .

---

**Algorithm 2 computeErrorIndicators**


---

**Input:** mesh  $\Delta t$ , Wiener path  $W$ .

**Output:** error indicators  $\bar{r}$ , path solutions  $\bar{X}$  and  $\bar{\varphi}_x$ , error density  $\bar{\rho}$ .

Compute the SDE path  $\bar{X}$  using the Euler–Maruyama method (4).

Compute the first variation  $\bar{\varphi}_x$  using the backward method (14).

Compute the error density  $\bar{\rho}$  and error indicators  $\bar{r}$  by the formulas (16) and (17), respectively.

---

**2.3. Numerical examples.** To illustrate the procedure for computing error indicators and the performance of the adaptive algorithm, we now present four SDE example problems. To keep matters relatively elementary, the dual solutions  $\varphi_x(t)$  for these examples are derived not from a *posteriori* but a *priori* analysis.

**Example 2.1.** We consider the classic geometric Brownian motion problem

$$dX_t = X_t dt + X_t dW_t, \quad X_0 = 1,$$

for which we seek to minimize the MSE

$$\mathbb{E}[(X_T - \bar{X}_T)^2] = \min!, \quad N \text{ given}, \quad (28)$$

at the final time  $T = 1$ , cf. the goal (B.1). One may derive that the dual solution of this problem is of the form

$$\varphi_x(X_t, t) = \partial_{X_t} X_T^{X_t, t} = \frac{X_T}{X_t},$$

which leads to the error density

$$\rho(t) = \frac{(b_x b)^2(X_t, t) \varphi_x(X_t, t)}{2} = \frac{X_T^2}{2}.$$

We conclude that uniform time stepping is optimal. A further reduction of the MSE could be achieved by allowing the number of time steps to depend on the final time magnitude of the realization. This is however outside the scope of the considered refinement goal (B.1), where we assume the number of time steps  $N$  is fixed for all realizations.

**Example 2.2.** Our second example is the two dimensional SDE problem

$$\begin{aligned} dW_t &= 1dW_t, & W_0 &= 0, \\ dX_t &= W_t dW_t, & X_0 &= 0. \end{aligned}$$

Here we seek to minimize the MSE  $E[(X_T - \bar{X}_T)^2]$  for the observable

$$X_T = \int_0^T W_t dW_t$$

at the final time  $T = 1$ . Representing the diffusion matrix by

$$b((W_t, X_t), t) = \begin{bmatrix} 1 \\ W_t \end{bmatrix},$$

and observing that

$$\partial_{X_t} X_T^{X_t, t} = \partial_{X_t} \left( X_t + \int_t^T W_s dW_s \right) = 1,$$

it follows from the error density in multi-dimensions in equation (65) that  $\rho(t) = \frac{1}{2}$ . We conclude that uniform time stepping is optimal for this problem as well.

**Example 2.3.** Next, we consider the 3D SDE problem

$$\begin{aligned} dW_t^{(1)} &= 1dW_t^{(1)}, & W_0^{(1)} &= 0, \\ dW_t^{(2)} &= 1dW_t^{(2)}, & W_0^{(2)} &= 0, \\ dX_t &= W_t^{(1)} dW_t^{(2)} - W_t^{(2)} dW_t^{(1)}, & X_0 &= 0, \end{aligned}$$

where  $W_t^{(1)}$  and  $W_t^{(2)}$  are independent Wiener processes. Here we seek to minimize the MSE  $E[(X_T - \bar{X}_T)^2]$  for the Levy area observable

$$X_T = \int_0^T (W_t^{(1)} dW_t^{(2)} - W_t^{(2)} dW_t^{(1)}),$$

at the final time  $T = 1$ . Representing the diffusion matrix by

$$b((W_t, X_t), t) = \begin{bmatrix} 1 & 0 \\ 0 & 1 \\ -W_t^{(1)} & W_t^{(2)} \end{bmatrix},$$

and observing that

$$\partial_{X_t} X_T^{X_t, t} = \partial_{X_t} \left( X_t + \int_t^T W_s dW_s \right) = 1,$$

it follows from equation (65) that  $\rho(t) = 1$ . We conclude that uniform time stepping is optimal for computing Levy areas.

**Example 2.4.** As the last example, we consider the 2D SDE

$$\begin{aligned} dW_t &= 1dW_t, & W_0 &= 0, \\ dX_t &= 3(W_t^2 - t)dW_t, & X_0 &= 0. \end{aligned}$$

We seek to minimize the MSE (28) at the final time  $T = 1$ . For this problem, it may be shown by Itô calculus that the pathwise exact solution is  $X_T = W_T^3 - 3W_T T$ . Representing the diffusion matrix by

$$b((W_t, X_t), t) = \begin{bmatrix} 1 \\ 3(W_t^2 - t) \end{bmatrix},$$

equation (65) implies that  $\rho(t) = 18W_t^2$ . This motivates using the discrete error indicators  $\bar{r}_n = 18W_{t_n}^2 \Delta t_n^2$  in the mesh refinement criterion. In Figure 2, we compare the uniform and adaptive time stepping Euler–Maruyama methods in terms of MSE vs. the number of time steps  $N$ . Estimates for the MSE for both methods are computed by an MC method using  $M = 10^6$  samples; a sufficient sample size to render the MC estimates’ statistical error negligible. For the adaptive

method, we have used the following input parameters in Algorithm 1: uniform input mesh  $\Delta t$  with step size  $2/N$  (and  $\Delta t_{\max} = 2/N$ ), and the number of refinements is set to  $N_{\text{refine}} = N/2$ . We observe that the methods have approximately equal convergence rates, but, as is to be expected, the adaptive algorithm is slightly more accurate than the uniform time stepping method.

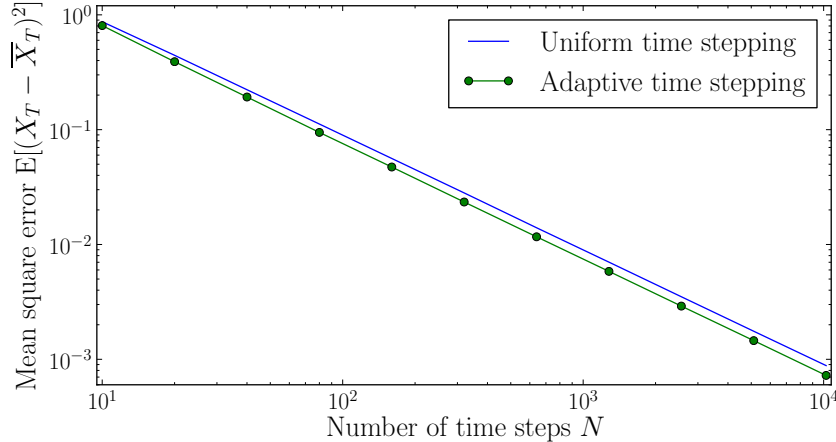


FIGURE 2. Comparison of the performance of uniform and adaptive time stepping Euler–Maruyama numerical integration for Example 2.4 in terms of MSE vs. number of time steps.

*Remark 2.3.* The error densities derived in the above examples can also be used in the error expansion (12) to achieve asymptotic error control of the MSE. See [29] for an approach on error control for weak approximations of SDE by means of the error density terms.

### 3. EXTENSION OF THE ADAPTIVE ALGORITHM TO THE MULTILEVEL SETTING

In this section, we incorporate the MSE adaptive time stepping algorithm presented in the preceding section into an MSE adaptive MLMC method for weak approximations. First, we shortly recall the approximation goal and important concepts for the MSE adaptive MLMC method, such as the structure of the adaptive mesh hierarchy and MLMC error control. Thereafter, the MLMC algorithm is presented in pseudocode form.

**3.1. Notation and objective.** For a tolerance  $\text{TOL} > 0$  and confidence  $0 < 1 - \delta < 1$ , we recall that our objective is to construct an adaptive time stepping MLMC estimator  $\mathcal{A}_{\text{MLC}}$  which meets the approximation constraint

$$\mathbb{P}(|\mathbb{E}[g(X_T)] - \mathcal{A}_{\text{MLC}}| \leq \text{TOL}) \geq 1 - \delta. \quad (29)$$

We denote the multilevel estimator by

$$\mathcal{A}_{\text{MLC}} := \sum_{\ell=0}^L \underbrace{\sum_{i=1}^{M_\ell} \frac{\Delta_\ell g(\omega_{i,\ell})}{M_\ell}}_{=: \mathcal{A}(\Delta_\ell g(\omega_{i,\ell}); M_\ell)}, \quad (30)$$

where

$$\Delta_\ell g(\omega_{i,\ell})(\omega) := \begin{cases} g(\overline{X}_T^{\{0\}}(\omega)), & \text{if } \ell = 0, \\ g(\overline{X}_T^{\{\ell\}}(\omega)) - g(\overline{X}_T^{\{\ell-1\}}(\omega)), & \text{else.} \end{cases}$$

See Section 1.2.5 for further details on MLMC notation and parameters.

3.1.1. *The mesh hierarchy.* A realization  $\Delta_\ell g(\omega_{i,\ell})$  is generated on a nested pair of mesh realizations

$$\dots \subset \Delta t^{\{\ell-1\}}(\omega_{i,\ell}) \subset \Delta t^{\{\ell\}}(\omega_{i,\ell}).$$

Mesh realizations are generated step by step from a prescribed and deterministic input mesh  $\Delta t^{\{-1\}}$  holding  $N_{-1}$  uniform time steps. First,  $\Delta t^{\{-1\}}$  is refined into a mesh  $\Delta t^{\{0\}}$  by calling Algorithm 1

$$[\Delta t^{\{0\}}, W^{\{0\}}] = \mathbf{meshRefinement} \left( \Delta t^{\{-1\}}, W^{\{-1\}}, N_{\text{refine}} = N_{-1}, \Delta t_{\text{max}} = N_0^{-1} \right).$$

Mesh refinement calls are iterated until the meshes  $\Delta t^{\{\ell-1\}}$  and  $\Delta t^{\{\ell-1\}}$  are produced, with the last couple of calls being

$$[\Delta t^{\{\ell-1\}}, W^{\{\ell-1\}}] = \mathbf{meshRefinement} \left( \Delta t^{\{\ell-2\}}, W^{\{\ell-2\}}, N_{\ell-2}, N_{\text{refine}} = N_{\ell-2}, \Delta t_{\text{max}} = N_{\ell-1}^{-1} \right),$$

and

$$[\Delta t^{\{\ell\}}, W^{\{\ell\}}] = \mathbf{meshRefinement} \left( \Delta t^{\{\ell-1\}}, W^{\{\ell-1\}}, N_{\ell-1}, N_{\text{refine}} = N_{\ell-1}, \Delta t_{\text{max}} = N_\ell^{-1} \right).$$

The output realization  $\Delta_\ell g(\omega_{i,\ell}) = g\left(\overline{X}_T^{\{\ell\}}(\omega_{i,\ell})\right) - g\left(\overline{X}_T^{\{\ell-1\}}(\omega_{i,\ell})\right)$  is thereafter generated on the output temporal mesh and Wiener path pairs  $(\Delta t^{\{\ell-1\}}, W^{\{\ell-1\}})$  and  $(\Delta t^{\{\ell\}}, W^{\{\ell\}})$ .

For later estimates of the computational cost of the MSE adaptive MLMC method, it is useful to have upper bounds on the growth of the number of time steps in the mesh hierarchy  $\{\Delta t^{\{\ell\}}\}_\ell$  as  $\ell$  increases. Letting  $|\Delta t|$  denote the number of time steps in a mesh  $\Delta t$  (i.e., the cardinality of the set  $\Delta t = \{\Delta t_0, \Delta t_1, \dots\}$ ), the following bounds hold

$$N_\ell \leq |\Delta t^{\{\ell\}}| < 2N_\ell \quad \forall \ell \in \mathbb{N}_0. \quad (31)$$

The lower bound follows straightforwardly from the mesh hierarchy refinement procedure described above. To show the upper bound, notice that the maximum number of mesh refinements going from a level  $\ell - 1$  mesh  $\Delta t^{\{\ell-1\}}$  to a level  $\ell$  mesh  $\Delta t^{\{\ell\}}$  is  $2N_{\ell-1} - 1$ . Consequently,

$$\begin{aligned} |\Delta t^{\{\ell\}}| &\leq |\Delta t^{\{-1\}}| + \sum_{j=0}^{\ell-1} \text{Maximum number of refinements going from } \Delta t^{\{j-1\}} \text{ to } \Delta t^{\{j\}} \\ &\leq N_{-1} + 2 \sum_{j=0}^{\ell} N_{j-1} - (\ell + 1) < 2N_\ell. \end{aligned}$$

*Remark 3.1.* For the telescoping property  $\mathbb{E}[\mathcal{A}_{\mathcal{MLC}}] = \mathbb{E}\left[g\left(\overline{X}_T^{\{\ell\}}\right)\right]$  to hold, it is not required that the adaptive mesh hierarchy is nested (but non-nested meshes make it more complicated to compute Wiener path pairs  $(W^{\{\ell-1\}}, W^{\{\ell\}})(\omega)$ ). In the numerical tests leading to this paper, we have tested both nested and non-nested adaptive meshes and found that both options perform satisfactorily.

3.2. **Error control.** The error control for the adaptive MLMC algorithm follows the general framework of uniform time step MLMC, but for the sake of completeness, we recall the error control framework for the setting of weak approximations. By splitting

$$|\mathbb{E}[g(X_T)] - \mathcal{A}_{\mathcal{MLC}}| \leq \underbrace{\left| \mathbb{E}\left[g(X_T) - g\left(\overline{X}_T^{\{L\}}\right)\right] \right|}_{=: \mathcal{E}_T} + \underbrace{\left| \mathbb{E}\left[g\left(\overline{X}_T^{\{L\}}\right) - \mathcal{A}_{\mathcal{MLC}}\right] \right|}_{=: \mathcal{E}_S}$$

and

$$\text{TOL} = \text{TOL}_T + \text{TOL}_S, \quad (32)$$

we seek to implicitly fulfil (29) through imposing the stricter constraints

$$\mathcal{E}_T \leq \text{TOL}_T, \quad \text{the time discretization error,} \quad (33)$$

$$P(\mathcal{E}_S \leq \text{TOL}_S) \geq 1 - \delta, \quad \text{the statistical error.} \quad (34)$$

3.2.1. *The statistical error.* Under the moment assumptions stated in [6], Lindeberg's version of the central limit theorem yields that as  $\text{TOL} \downarrow 0$ ,

$$\frac{\mathcal{A}_{\mathcal{M}\mathcal{L}} - \mathbb{E}\left[g\left(\overline{X}_T^{(L)}\right)\right]}{\sqrt{\text{Var}(\mathcal{A}_{\mathcal{M}\mathcal{L}})}} \xrightarrow{D} N(0, 1). \quad (35)$$

Here,  $\xrightarrow{D}$  denotes convergence in distribution and by construction we have

$$\text{Var}(\mathcal{A}_{\mathcal{M}\mathcal{L}}) = \sum_{\ell=0}^L \frac{\text{Var}(\Delta_\ell g)}{M_\ell}.$$

This asymptotic result motivates the statistical error constraint

$$\text{Var}(\mathcal{A}_{\mathcal{M}\mathcal{L}}) \leq \frac{\text{TOL}_S^2}{C_C^2}, \quad (36)$$

where  $C_C(\delta)$  is the confidence parameter chosen so that

$$1 - \frac{1}{\sqrt{2\pi}} \int_{-C_C}^{C_C} e^{-x^2/2} dx = (1 - \delta), \quad (37)$$

for a prescribed confidence  $(1 - \delta)$ .

Another important question is how to distribute the number of samples  $\{M_\ell\}_\ell$  on the level hierarchy so that both the computational cost of the MLMC estimator is minimized and the constraint (36) is met. Letting  $C_\ell$  denote the expected cost of generating a numerical realization  $\Delta_\ell g(\omega_{i,\ell})$ , the approximate total cost of generating the multilevel estimator becomes

$$\mathcal{C}_{\mathcal{M}\mathcal{L}} := \sum_{\ell=0}^L C_\ell M_\ell.$$

An optimization of the number of samples at each level can then be found through minimization of the Lagrangian

$$\mathcal{L}(M_0, M_1, \dots, M_L, \lambda) = \lambda \left( \sum_{\ell=0}^L \frac{\text{Var}(\Delta_\ell g)}{M_\ell} - \frac{\text{TOL}_S^2}{C_C^2} \right) + \sum_{\ell=0}^L C_\ell M_\ell,$$

yielding

$$M_\ell = \left\lceil \frac{C_C^2}{\text{TOL}_S^2} \sqrt{\frac{\text{Var}(\Delta_\ell g)}{C_\ell}} \sum_{\ell=0}^L \sqrt{C_\ell \text{Var}(\Delta_\ell g)} \right\rceil, \quad \ell = 0, 1, \dots, L.$$

Since the cost of adaptively refining a mesh  $\Delta t^{(\ell)}$  is  $\mathcal{O}(N_\ell \log(N_\ell)^2)$ , as noted in Section 2.2.3, the cost of generating an SDE realization is of the same order;  $C_\ell = \mathcal{O}(N_\ell \log(N_\ell)^2)$ . Representing the cost by its leading order term and disregarding the logarithmic factor, an approximation to the level-wise optimal number of samples becomes

$$M_\ell = \left\lceil \frac{C_C^2}{\text{TOL}_S^2} \sqrt{\frac{\text{Var}(\Delta_\ell g)}{N_\ell}} \sum_{\ell=0}^L \sqrt{N_\ell \text{Var}(\Delta_\ell g)} \right\rceil, \quad \ell = 0, 1, \dots, L. \quad (38)$$

*Remark 3.2.* In our MLMC implementations, the variances  $\text{Var}(\Delta_\ell g)$  in equation (38) are approximated by sample variances. To save memory in our parallel computer implementation, the maximum permitted batch size for a set of realizations  $\{\Delta_\ell g(\omega_{i,\ell})\}_i$  is set to 100000. For the initial batch consisting of  $M_\ell = \widehat{M}$  samples, the sample variance is computed by the standard approach

$$\mathcal{V}(\Delta_\ell g; M_\ell) = \frac{1}{M_\ell - 1} \sum_{i=1}^{M_\ell} (\Delta_\ell g(\omega_{i,\ell}) - \mathcal{A}(\Delta_\ell g; M_\ell))^2.$$

Thereafter, for every new batch of realizations  $\{\Delta_\ell g(\omega_{i,\ell})\}_{i=M_\ell+1}^{M_\ell+M}$  ( $M$  here denoting an arbitrary natural number smaller or equal to 100000), we incrementally update the sample variance,

$$\begin{aligned} \mathcal{V}(\Delta_\ell g; M_\ell + M) &= \frac{M_\ell}{M_\ell + M} \times \mathcal{V}(\Delta_\ell g; M_\ell) \\ &+ \frac{1}{(M_\ell + M - 1)} \sum_{i=M_\ell+1}^{M_\ell+M} (\Delta_\ell g(\omega_{i,\ell}) - \mathcal{A}(\Delta_\ell g; M_\ell + M))^2, \end{aligned}$$

and update the total number of samples on level  $\ell$  accordingly,  $M_\ell = M_\ell + M$ .

**3.2.2. The time discretization error.** For controlling the time discretization error, we assume a weak order convergence rate  $\alpha > 0$  holds for the given SDE problem when solved with the Euler-Maruyama method, i.e.,

$$\left| \mathbb{E} \left[ g(X_T) - g(\bar{X}_T^{(L)}) \right] \right| = \mathcal{O}(N_L^{-\alpha}),$$

and we assume that the asymptotic rate is reached at level  $L - 1$ . Then

$$\left| \mathbb{E} \left[ g(X_T) - g(\bar{X}_T^{(L)}) \right] \right| = \left| \sum_{\ell=L+1}^{\infty} \mathbb{E}[\Delta_\ell g] \right| \leq |\mathbb{E}[\Delta_L g]| \sum_{\ell=L+1}^{\infty} 2^{-\alpha\ell} = \frac{|\mathbb{E}[\Delta_L g]|}{2^\alpha - 1}.$$

In our implementation, we assume the weak convergence rate  $\alpha$  is known prior to sampling and, replacing  $\mathbb{E}[\Delta_L g]$  by a sample average approximation in the above inequality, we determine  $L$  by the following stopping criterion:

$$\frac{\max(2^{-\alpha} |\mathcal{A}(\Delta_{L-1} g; M_{L-1})|, |\mathcal{A}(\Delta_L g; M_L)|)}{2^\alpha - 1} \leq \text{TOL}_T, \quad (39)$$

cf. Algorithm 3. A final level  $L$  of order  $\log(\text{TOL}_T^{-1})$  will thus control the discretization error.

**3.2.3. Computational cost.** Under the convergence rate assumptions stated in Theorem 1.1, it follows that the cost of generating an adaptive MLMC estimator  $\mathcal{A}_{\mathcal{M}\mathcal{L}}$  fulfilling the MSE approximation goal  $\mathbb{E}[(\mathcal{A}_{\mathcal{M}\mathcal{L}} - \mathbb{E}[g(X_T)])^2] \leq \text{TOL}^2$  is bounded by

$$\mathcal{C}_{\mathcal{M}\mathcal{L}} = \sum_{\ell=0}^L M_\ell C_\ell \leq \begin{cases} \mathcal{O}(\text{TOL}^{-2}), & \text{if } \beta > 1, \\ \mathcal{O}(\text{TOL}^{-2} \log(\text{TOL})^4), & \text{if } \beta = 1, \\ \mathcal{O}(\text{TOL}^{-2 + \frac{\beta-1}{\alpha}} \log(\text{TOL})^2), & \text{if } \beta < 1. \end{cases} \quad (40)$$

Moreover, under the additional higher moment approximation rate assumption  $\mathbb{E} \left[ g(\bar{X}_T^{(\ell)}) - g(X_T) \right]^{2+\nu} = \mathcal{O}(2^{-\beta+\nu/2})$ , the complexity bound (40) also holds for fulfilling criterion (2), asymptotically as  $\text{TOL} \downarrow 0$ , cf. [5].

**3.3. MLMC pseudocode.** In this section, we present pseudocode for the implementation of the MSE adaptive MLMC method. In addition to Algorithms 1 and 2, presented in Section 2.2.4, the implementation consists of Algorithms 3 and 4. Algorithm 3 describes how the stopping criterion for the final level  $L$  is implemented and how the multilevel estimator is generated, and Algorithm 4 describes the steps for generating a realization  $\Delta_\ell g(\omega)$ .

*Remark 3.3.* For each increment of  $L$  in Algorithm 3, all realizations  $\Delta_\ell g(\omega_{i,\ell})$  that have been generated up to that point are reused in later computations of the multilevel estimator. This approach, which is common in MLMC, cf. [8], seems to work fine in practice although the independence between samples then is lost (which again makes the resulting convergence analysis more complicated).

---

**Algorithm 3** mlmcEstimator

---

**Input:**  $\text{TOL}_T$ ,  $\text{TOL}_S$ , confidence  $\delta$ , initial mesh  $\Delta t^{\{-1\}}$ , initial number of mesh steps  $N_{-1}$ , input weak rate  $\alpha$ , initial number of samples  $\widehat{M}$ .

**Output:** Multilevel estimator  $\mathcal{A}_{\mathcal{MLC}}$ .

Compute the confidence parameter  $C_C(\delta)$  by (37).

Set  $L = -1$ .

**while**  $L < 2$  **or** (39), using the input  $\alpha$ , is violated **do**

  Set  $L = L + 1$ .

  Set  $M_L = \widehat{M}$ , generate a set of realizations  $\{\Delta_\ell g(\omega_{i,\ell})\}_{i=1}^{M_L}$  by calling **adaptiveRealizations**( $\Delta t^{\{-1\}}$ ).

**for**  $\ell = 0$  **to**  $L$  **do**

    Compute the sample variance  $\mathcal{V}(\Delta_\ell g; M_\ell)$ .

**end for**

**for**  $\ell = 0$  **to**  $L$  **do**

    Determine the number of samples  $M_\ell$  by (38).

**if** new value of  $M_\ell$  is larger than the old value **then**

      Compute additional realizations  $\{\Delta_\ell g(\omega_{i,\ell})\}_{i=M_\ell+1}^{M_\ell^{new}}$  by calling **adaptiveRealizations**( $\Delta t^{\{-1\}}$ ).

**end if**

**end for**

**end while**

Compute  $\mathcal{A}_{\mathcal{MLC}}$  from the generated samples by using formula (7).

---



---

**Algorithm 4** adaptiveRealization

---

**Input:** Mesh  $\Delta t^{\{-1\}}$ .

**Outputs:** One realization  $\Delta_\ell g(\omega)$

Generate a wiener path  $W^{\{-1\}}$  on the initial mesh  $\Delta t^{\{-1\}}$ .

**for**  $j = 0$  **to**  $\ell$  **do**

  Refine the mesh by calling

$$[\Delta t^{\{j\}}, W^{\{j\}}] = \mathbf{meshRefinement}(\Delta t^{\{j-1\}}, W^{\{j-1\}}, N_{\text{refine}} = N_{j-1}, \Delta t_{\text{max}} = N_j^{-1}).$$

**end for**

Compute Euler–Maruyama realizations  $(\overline{X}_T^{\{\ell-1\}}, \overline{X}_T^{\{\ell\}})(\omega)$  using the mesh pair  $(\Delta t^{\{\ell-1\}}, \Delta t^{\{\ell\}})(\omega)$  and Wiener path pair  $(W^{\{\ell-1\}}, W^{\{\ell\}})(\omega)$ , cf. (4), and return the output

$$\Delta_\ell g(\omega) = g\left(\overline{X}_T^{\{\ell\}}(\omega)\right) - g\left(\overline{X}_T^{\{\ell-1\}}(\omega)\right).$$


---

## 4. NUMERICAL EXAMPLES FOR THE MLMC METHODS

To illustrate the implementation of the MSE adaptive MLMC method and show its potential efficiency gain over the uniform MLMC method, two numerical examples are presented in this section. The first example considers a geometric Brownian motion SDE problem with sufficient regularity, so that there is very little (probably nothing) to gain by introducing adaptive mesh refinement. The example is included to show that in settings where adaptivity is not required, the MSE adaptive MLMC method is not excessively more expensive than the uniform MLMC method. In the second example, we consider an SDE with a random time drift coefficient blow-up of order  $t^{-p}$  with  $p \in [0.5, 1)$ . The MSE adaptive MLMC method performs progressively more efficiently than the uniform MLMC method the higher the value of the blow-up exponent  $p$  takes.

For reference, the implemented MSE adaptive MLMC method is described in Algorithms 1–4, the standard form of the uniform time step MLMC method that we use in these numerical

comparisons is presented in Algorithm 5, Appendix B, and a summary of the parameter values used in the examples is given in Table 2. Furthermore, all average properties derived from the MLMC methods that we plot for the considered examples in Figures 3–12 below are computed from 100 multilevel estimator realizations, and, when plotted, error bars are scaled to one sample standard deviation.

TABLE 2. List of parameter values used by the MSE adaptive MLMC method and (when required) the uniform MLMC method in the implemented numerical examples in Section 4.

| Parameter               | Description of parameter   | Example 4.1   | Example 4.2   |
|-------------------------|--|---|---|
| $\delta$                | Confidence parameter, cf. (29).  | 0.1   | 0.1   |
| TOL                     | Accuracy parameter, cf. (29).  | $[10^{-3}, 10^{-1}]$                                    | $[10^{-3}, 10^{-1}]$                                    |
| TOL <sub>S</sub>        | Statistical error tolerance, cf. (32).   | TOL/2   | TOL/2   |
| TOL <sub>T</sub>        | Bias error tolerance, cf. (32).  | TOL/2   | TOL/2   |
| $\Delta t^{\{-1\}}$     | Pre-initial input uniform mesh having the following step size.   | 1/2   | 1/2   |
| $N_0$                   | Number of time steps in the initial mesh $\Delta t^{\{0\}}$ .  | 4   | 4   |
| $\tilde{N}(\ell)$       | The number of complete updates of the error indicators in the MSE adaptive method, cf. Algorithm 1.                                  | $\left\lceil \frac{\log(\ell+2)}{\log(2)} \right\rceil$ | $\left\lceil \frac{\log(\ell+2)}{\log(2)} \right\rceil$ |
| $\Delta t_{\max}(\ell)$ | Maximum permitted time step size.  | $N_\ell^{-1}$   | $N_\ell^{-1}$   |
| $\Delta t_{\min}$       | Minimum permitted time step size (due to the used double-precision binary floating-point format).                                    | $2^{-51}$   | $2^{-51}$   |
| $\widehat{M}$           | Number of first batch samples for a (first) estimate of the variance $\text{Var}(\Delta_\ell g)$ .                                   | 100   | 20  |
| $\alpha_U$              | Input weak convergence rate required for the stopping rule (39) for uniform time step Euler–Maruyama numerical integration.          | 1   | $(1-p)$   |
| $\alpha_A$              | Input weak convergence rate required for the stopping rule (39) for the MSE adaptive time step Euler–Maruyama numerical integration, | 1   | 1   |

**Example 4.1.** We consider the classical geometric Brownian motion

$$dX_t = X_t dt + X_t dW_t, \quad X_0 = 1, \quad (41)$$

where we seek to fulfill the weak approximation goal (2) for the observable  $g(x) = x$  at the final time  $T = 1$ . The reference solution is  $\mathbb{E}[g(X_T)] = e^T$ . From Example 2.1, we recall that the

MSE minimized for this problem by using uniform time steps. However, our *a posteriori* MSE adaptive MLMC method computes error indicators from numerical solutions of the path and the dual solution, which may lead to slightly non-uniform output meshes. In Figure 3, we study how close to uniform the MSE adaptive meshes are by plotting the level-wise ratio  $E[|\Delta t^{\{\ell\}}|]/N_\ell$ , where we recall that  $|\Delta t^{\{\ell\}}|$  denotes the number of time steps in the mesh  $\Delta t^{\{\ell\}}$  and that a uniform mesh on level  $\ell$  has  $N_\ell$  time steps. As the level  $\ell$  increases,  $E[|\Delta t^{\{\ell\}}|]/N_\ell$  converges to 1, and to interpret this result, we recall from the construction of the adaptive mesh hierarchy in Section 3 that if  $|\Delta t^{\{\ell\}}| = N_\ell$ , then the mesh  $\Delta t^{\{\ell\}}$  is uniform. We thus conclude that for this problem, the higher the level the more uniform the MSE adaptive mesh realizations generally become.

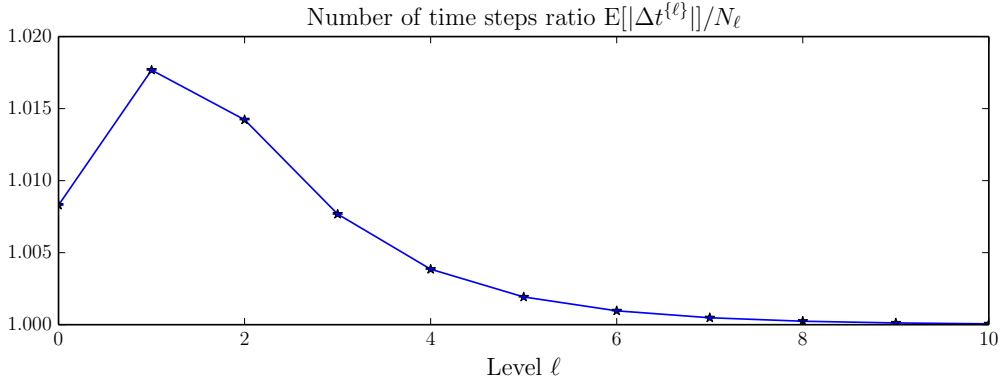


FIGURE 3. Level-wise mean number of time steps ratio  $E[|\Delta t^{\{\ell\}}|]/N_\ell$  of MSE adaptive mesh realizations to uniform mesh realizations for Example 4.2.

Since adaptive mesh refinement is costly and since this problem has sufficient regularity for the first order weak and MSE convergence rates (5) and (6) to hold, respectively, it is to be expected that for this example, MSE adaptive MLMC will be less efficient than the uniform MLMC. This is verified in Figure 5, which shows that runtime of MSE adaptive MLMC method grows slightly faster than the uniform MLMC method and that the cost ratio is at most roughly 3.5, in favor of uniform MLMC. In Figure 4, the accuracy of the MLMC methods is compared, showing that both methods fulfill the goal (2) reliably. Figure 6 further shows that both methods have roughly first order convergence rates for the weak error  $|E[\Delta_\ell g]|$  and the variance  $\text{Var}(\Delta_\ell g)$ , and that the decay rates for  $M_\ell$  are close to identical. We conclude that although MSE adaptive MLMC is slightly more costly than uniform MLMC, the methods perform quite similarly for this example.

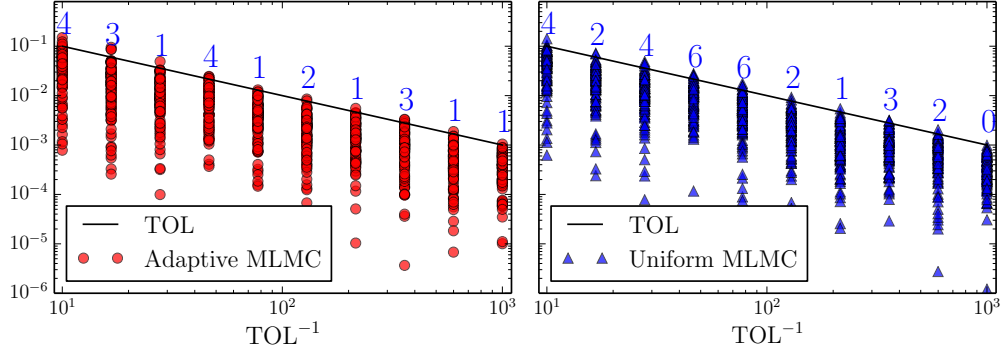


FIGURE 4. For a set of TOL values, 100 realizations of the MSE adaptive multilevel estimator is computed using both MLMC methods for Example 4.1. The errors  $|\mathcal{A}_{\mathcal{MLC}}(\omega_i; \text{TOL}, \delta) - \mathbb{E}[g(X_T)]|$  are respectively plotted as bullets (adaptive MLMC) and triangles (uniform MLMC), and the number of multilevel estimator realizations failing the constraint  $|\mathcal{A}_{\mathcal{MLC}}(\omega_i; \text{TOL}, \delta) - \mathbb{E}[g(X_T)]| < \text{TOL}$  is written above the  $(\text{TOL}^{-1}, \text{TOL})$  line. Since the confidence parameter is set to  $\delta = 0.1$  and less than 10 realizations fail for any of the tested TOL values, both methods meet the approximation goal (29).

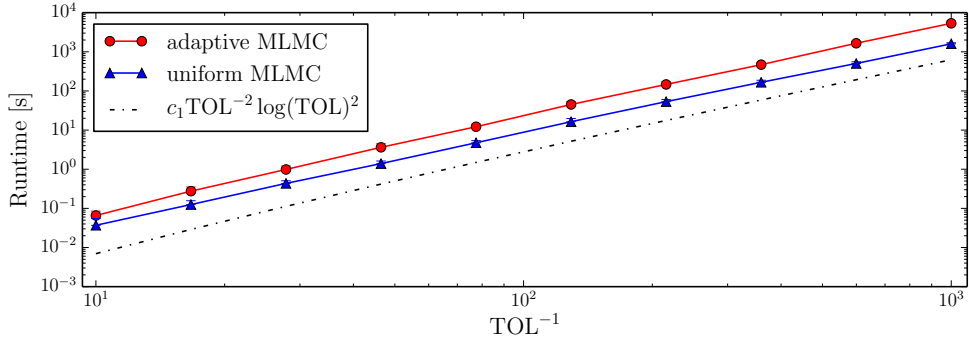


FIGURE 5. Average runtime vs.  $\text{TOL}^{-1}$  for the two MLMC methods solving Example 4.1.

**Example 4.2.** We next consider the SDE

$$\begin{aligned} dX_t &= \underbrace{r f_\xi(t) X_t}_{=: a(X_t, t)} dt + \underbrace{\sigma X_t}_{=: b(X_t, t)} dW_t \\ X_0 &= 1, \end{aligned} \quad (42)$$

with the low-regularity drift coefficient  $f_\xi(t) = |t - \xi|^{-p}$ , interest rate  $r = 1/5$ , volatility  $\sigma = 0.5$ , and observable  $g(x) = x$  at the final time  $T = 1$ . A new singularity point  $\xi \in U(1/4, 3/4)$  is sampled for each path, and it is independent from the Wiener paths  $W$ . Three different blow-up exponent test cases are considered,  $p = (1/2, 2/3, 3/4)$ , and to avoid blow-ups in the numerical integration of the drift function  $f_\xi$ , we replace the fully explicit Euler–Maruyama integration scheme with the following semi-implicit scheme:

$$\bar{X}_{n+1} = \begin{cases} r f_\xi(t_n) \bar{X}_n \Delta t_n + \sigma \bar{X}_n \Delta W_n, & \text{if } f_\xi(t_n) < 2f_\xi(t_{n+1}), \\ r f_\xi(t_{n+1}) \bar{X}_n \Delta t_n + \sigma \bar{X}_n \Delta W_n, & \text{else.} \end{cases} \quad (43)$$

For  $p \in [1/2, 3/4]$  it may be shown that for any singularity point, any path integrated by the scheme (43) will have at most one drift-implicit integration step. The reference mean for the exact

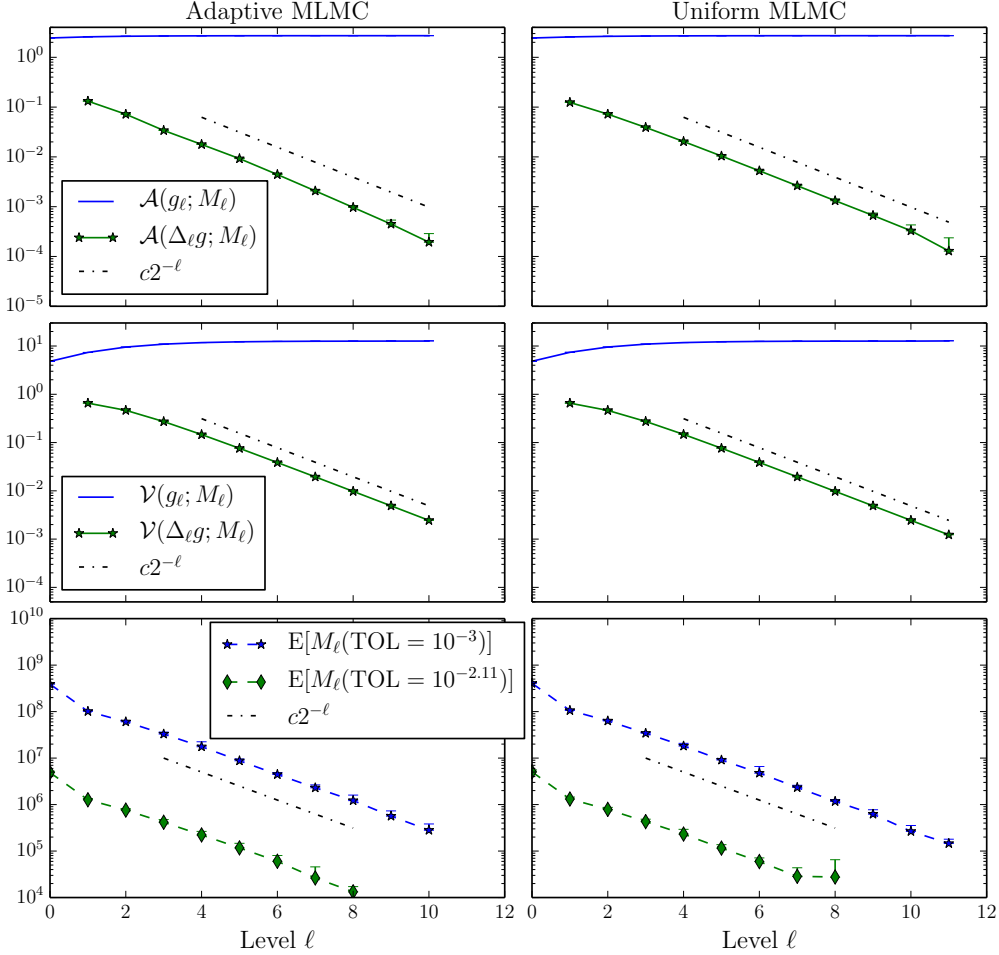


FIGURE 6. Output for Example 4.1 solved with the MSE adaptive- and uniform time step MLMC methods. **(Top)** Weak error  $|E[\Delta_{\ell}g]|$  for solutions at  $\text{TOL} = 10^{-3}$ . **(Middle)** Variance  $\text{Var}(\Delta_{\ell}g)$  for solutions at  $\text{TOL} = 10^{-3}$ . **(Bottom)** Average number of samples  $E[M_{\ell}]$ .

solution is given by

$$E[X_T] = 2 \int_{1/4}^{3/4} \exp\left(\frac{r(x^{1-p} + (1-x)^{1-p})}{1-p}\right) dx, \quad (44)$$

and in the numerical experiments, we approximate this integral value by quadrature to the needed accuracy.

*The MSE expansion for the adaptive method.* Due to the low-regularity drift present in this problem, the resulting MSE expansion will also contain drift related terms which formally are of higher order. From the proof of Theorem 2.1, equation (59), we conclude that to leading order, the MSE is bounded by

$$E\left[|\bar{X}_T - X_T|^2\right] \leq E\left[\sum_{n=0}^{N-1} \bar{\varphi}_{x,n+1}^2 \frac{(N(a_t + a_x a)^2 \Delta t_n^2 + b_x b^2)(\bar{X}_n, t_n)}{2} \Delta t_n^2\right]. \quad (45)$$

This is the error expansion we use for the adaptive mesh refinement (in Algorithm 1) in this example. In Figure 7 we illustrate the effect the singularity exponent  $p$  has on SDE- and adaptive mesh realizations.

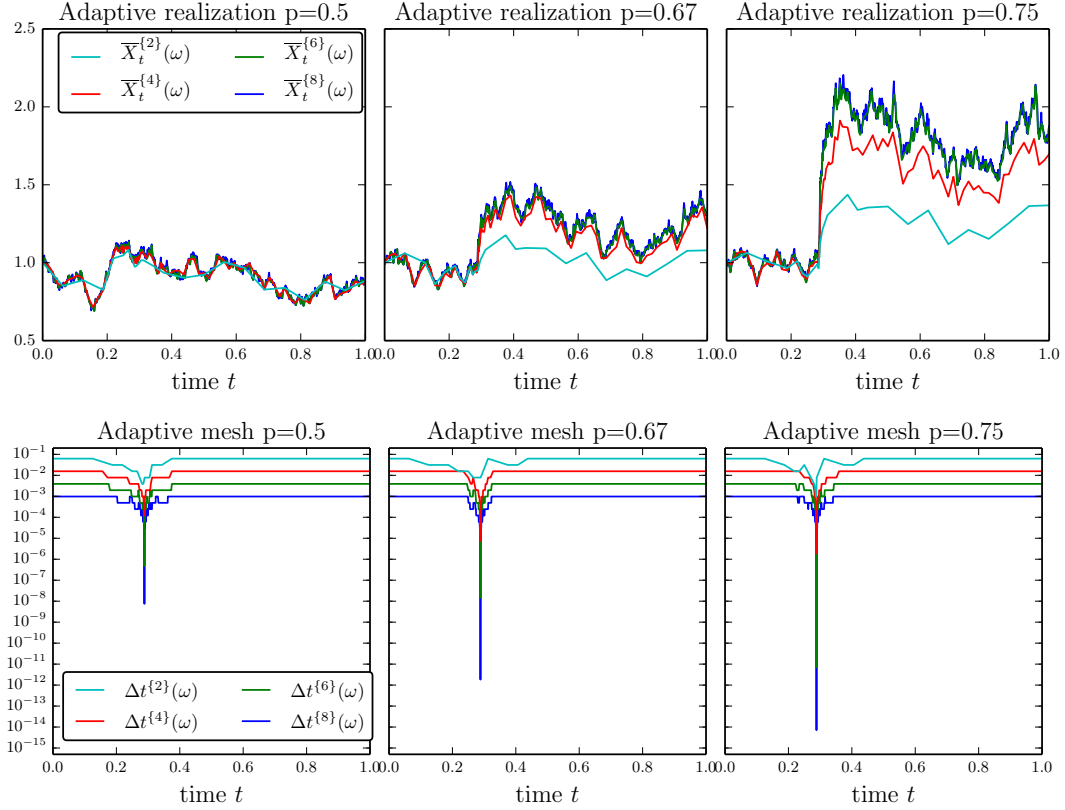


FIGURE 7. **(Top)** One MSE adaptive numerical realization of the SDE problem (42) at different mesh hierarchy levels. The blow-up singularity point is located at  $\xi = 0.288473\dots$  and the realizations are computed for three different singularity exponent values. We observe that the higher-valued the exponent  $p$  is, the more pronounced does the path's jump at  $t = \xi$  become. **(Bottom)** Corresponding MSE adaptive mesh realizations for the different test cases.

*Implementation details and observations.* Computational tests for the uniform and MSE adaptive MLMC methods are implemented with the input parameters summarized in Table 2. The weak convergence rate  $\alpha$ , which is needed in the MLMC implementations' stopping criterion (39), is estimated experimentally to  $\alpha(p) = (1 - p)$  when using Euler-Maruyama with uniform time steps, and roughly  $\alpha = 1$  when using Euler-Maruyama with adaptive time steps, cf. Figure 8. We further estimate the variance convergence rate to  $\beta(p) = 2(1 - p)$  when using uniform time stepping, and roughly  $\beta = 1$  when using MSE adaptive time stepping, cf. Figure 9. The low weak convergence rate for uniform MLMC implies that the number of levels  $L$  in the MLMC estimator will become very large, even for fairly high tolerances. Since computations of realizations on high levels are extremely costly, we have, for the sake of computational feasibility, chosen the very low value  $\widehat{M} = 20$  for the initial number of samples in both MLMC methods. The respective estimators' use of samples  $M_\ell$ , cf. Figure 10, shows that the low number of initial samples is not strictly needed for the adaptive MLMC method, but for the sake of fair comparisons, we have chosen to use the same parameter values in both methods.

From the rate estimates of  $\alpha$  and  $\beta$ , we predict the computational cost of reaching the approximation goal (29) for the respective MLMC methods to

$$\text{Cost}_{\text{adp}}(\mathcal{A}_{\mathcal{MLC}}) = \mathcal{O}(\log(\text{TOL})^4 \text{TOL}^{-2}) \quad \text{and} \quad \text{Cost}_{\text{unf}}(\mathcal{A}_{\mathcal{MLC}}) = \mathcal{O}\left(\text{TOL}^{-\frac{1}{1-p}}\right),$$

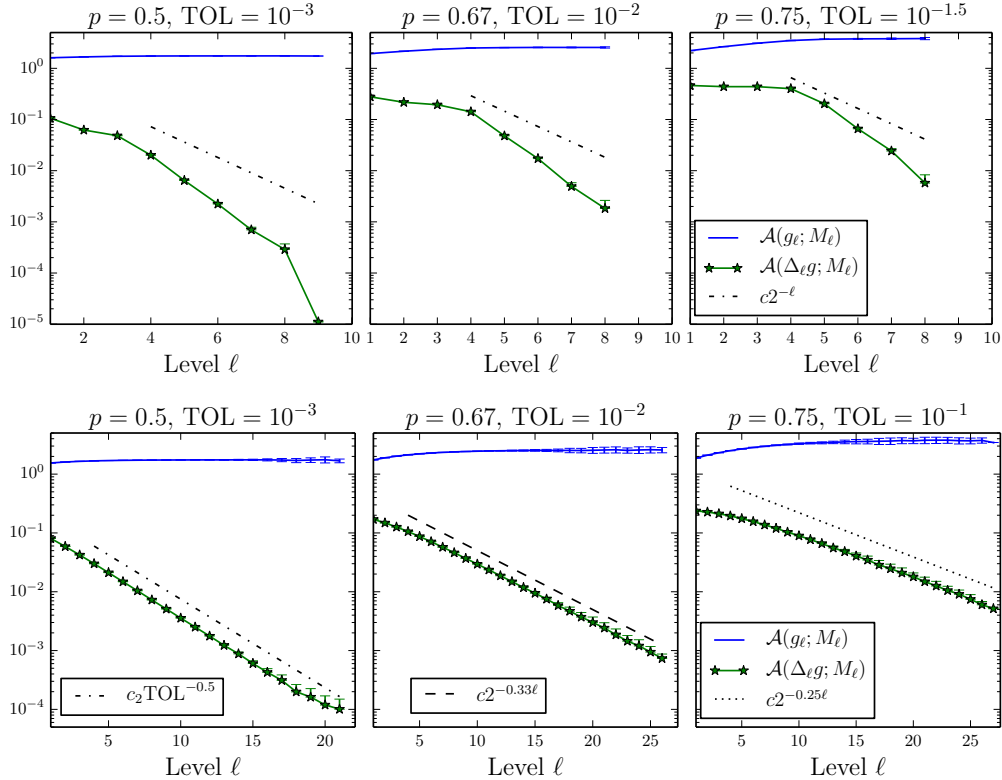


FIGURE 8. **(Top)** Average errors  $|\mathbb{E}[\Delta_\ell g]|$  for Example 4.2 solved with the MSE adaptive MLMC method for three different singularity exponent values. **(Bottom)** Corresponding average errors for the uniform MLMC method.

by using respectively the estimate (40) and Theorem 1.1. These predictions fit well with the observed computational runtime for the respective MLMC methods, cf. Figure 11. Lastly, we observe numerical results consistent with both methods fulfilling the goal (29) in Figure 12.

**Computer implementation.** The computer code for all algorithms was written in Java and used the “Stochastic Simulation in Java” library to sample the r.v. in parallel from thread-independent **MRG32k3a** pseudo random number generators, cf. [22]. The experiments were run on multiple threads on Intel Xeon(R) CPU X5650, 2.67GHz processors and the computer graphics were made using the open source plotting library Matplotlib, cf. [16].

## 5. CONCLUSION

We have developed an *a posteriori* MSE adaptive Euler–Maruyama time stepping method and incorporated it into an MSE adaptive MLMC method. The MSE error expansion presented in Theorem 2.1 was the fundament for the adaptive method. Numerical tests have shown that MSE adaptive time stepping may substantially outperform uniform time stepping, both in the single-level MC setting and in the MLMC setting, cf. Examples 2.4 and 4.2. Due to the complexities of implementing adaptive time stepping, the numerical examples in this paper were restricted to quite simple low-regularity SDE problems with singularities in the temporal coordinate. In the future, we aim to also study SDE problems with low-regularity in the state coordinate (preliminary tests and analysis do however indicate that then some ad hoc molding of the adaptive algorithm is required).

Although *a posteriori* adaptivity has proven to be a very effective method for deterministic differential equations, the use of information from the future of the numerical solution of the dual

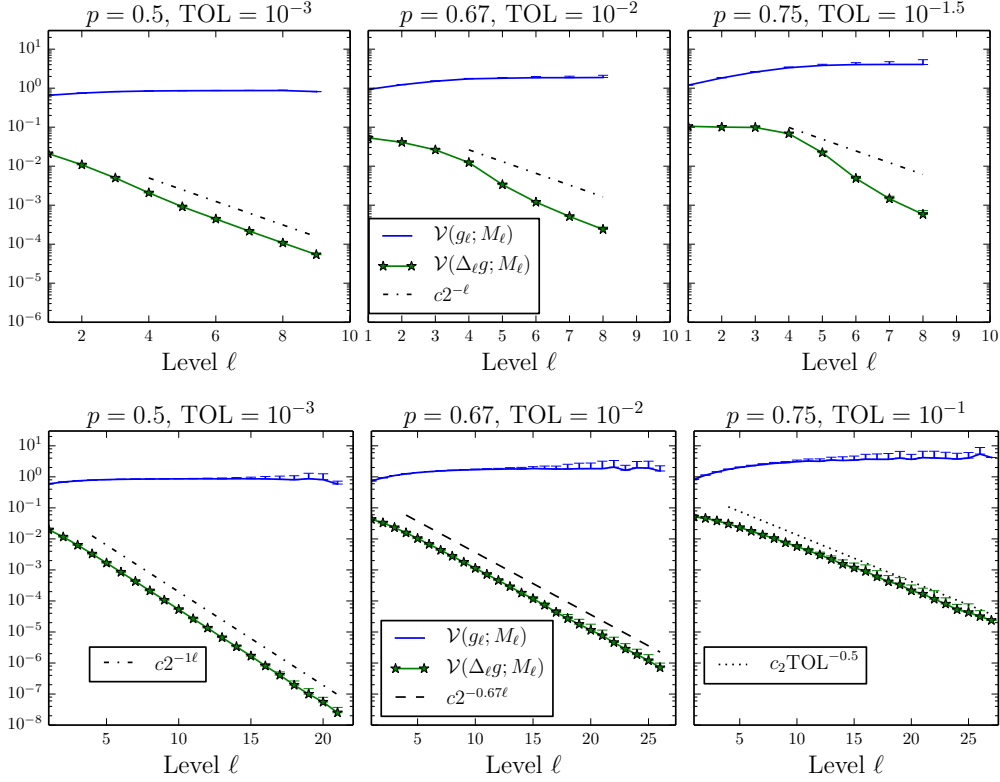


FIGURE 9. **(Top)** Variances  $\text{Var}(\Delta_\ell g)$  for for Example 4.2 solved with the MSE adaptive MLMC method for three different singularity exponent values. **(Bottom)** Corresponding variances for the uniform MLMC method. The more noisy the data on the highest levels is due to the low number used for the initial samples,  $\hat{M} = 20$ , and that only a subset the gene100 multilevel estimator realizations reached the last levels.

problem makes it a somewhat unnatural method to extend to Itô SDE: It can result in numerical solutions which are not  $\mathcal{F}_t$ -adapted, which consequently may introduce a bias in the numerical solutions. See [7] for an example of a failing adaptive method for SDE. A rigorous analysis of convergence properties of our developed MSE adaptive method would strengthen the method's theoretical basis further. We leave this as future work.

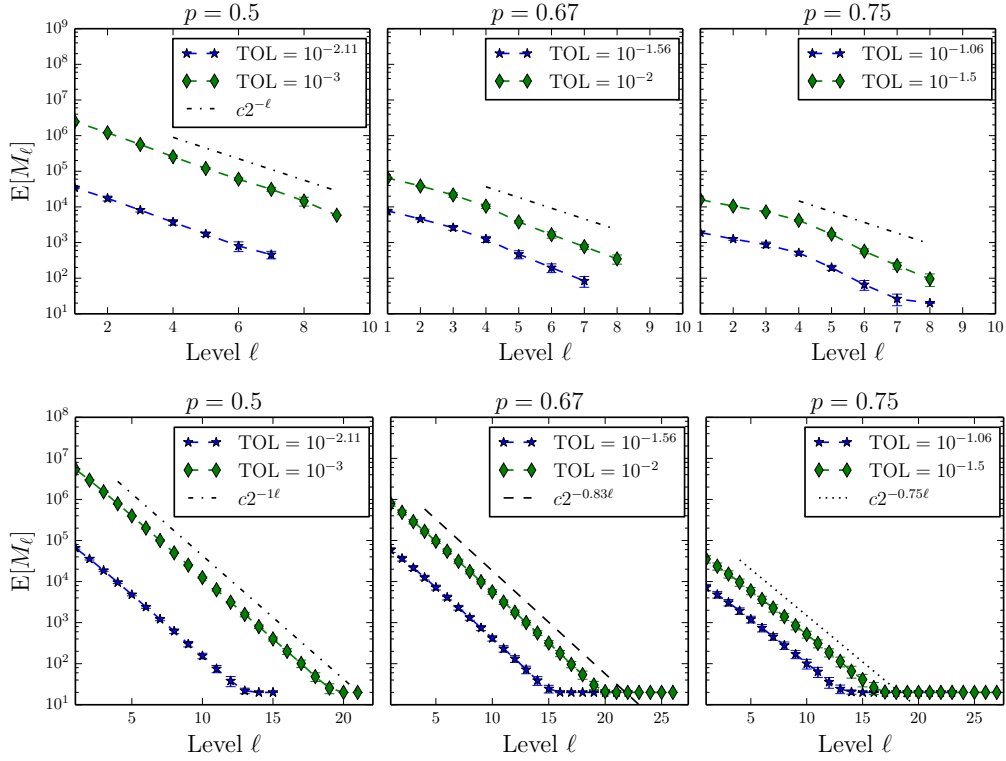


FIGURE 10. **(Top)** Average number of samples  $M_\ell$  for for Example 4.2 solved with the MSE adaptive MLMC method for three different singularity exponent values. **(Bottom)** Corresponding average number of samples for the uniform MLMC method. The plotted decay rate reference lines  $c2^{-((\beta(p)+1)/2)\ell}$  for  $M_\ell$  follows implicitly from equation (38) (assuming that  $\beta(p) = 2(1-p)$  is the correct variance decay rate).

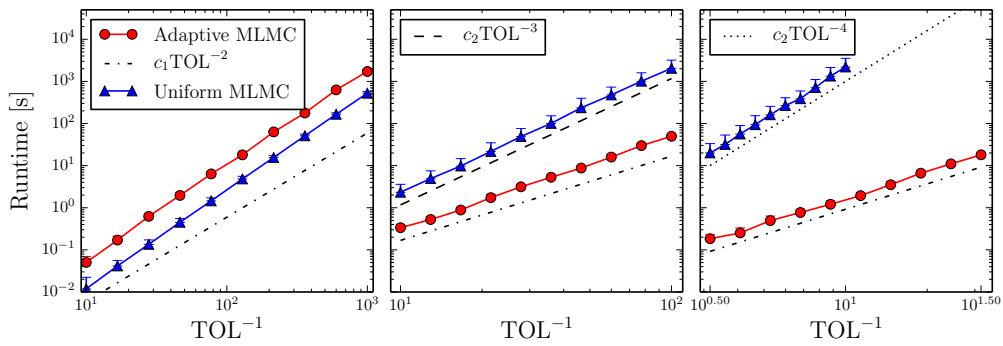


FIGURE 11. Average runtime vs.  $\text{TOL}^{-1}$  for the two MLMC methods for three different singularity exponent values in Example 4.2.

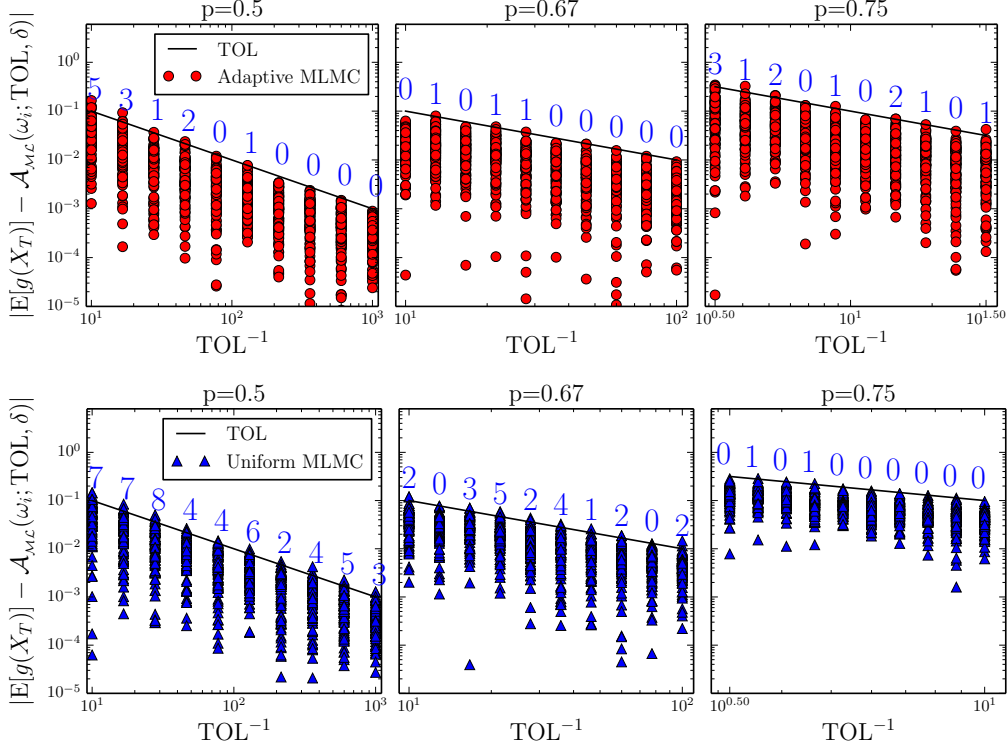


FIGURE 12. Approximation errors for both of the MLMC methods solving Example 4.2. At every TOL value, bullets and triangles represent the errors from 100 independent multilevel estimator realizations of the respective methods.

APPENDIX A. PROOFS

A.1. **Error expansion for the MSE in 1D.** In this section, we derive a leading order error expansion for the MSE (11) in the 1D setting when the drift and diffusion coefficients respectively are mappings of the form  $a : \mathbb{R} \times [0, T] \rightarrow \mathbb{R}$  and  $b : \mathbb{R} \times [0, T] \rightarrow \mathbb{R}$ . We begin by deriving a representation of the MSE in terms of products of local errors and weights.

First, we recall that  $X_T^{x,t}$  denotes a solution of the SDE (1) conditioned that  $X_t = x$ ,  $X_T$  is shorthand for  $X_T^{x_0,0}$ , and  $\varphi(x,t) := g(X_T^{x,t})$ . By the mean value theorem,

$$\begin{aligned}
 g(X_T) - g(\bar{X}_T) &= \varphi(x_0, 0) - \varphi(\bar{X}_T, T) \\
 &= \sum_{n=0}^{N-1} \varphi(\bar{X}_n, t_n) - \varphi(\bar{X}_{n+1}, t_{n+1}) \\
 &= \sum_{n=0}^{N-1} \varphi(X_{t_{n+1}}^{\bar{X}_n, t_n}, t_{n+1}) - \varphi(\bar{X}_{n+1}, t_{n+1}) \\
 &= \sum_{n=0}^{N-1} \varphi_x(\bar{X}_{n+1} + s_n \Delta e_n, t_{n+1}) \Delta e_n,
 \end{aligned}
 \tag{46}$$

where the *local error* is given by  $\Delta e_n := X_{t_{n+1}}^{\bar{X}_n, t_n} - \bar{X}_{n+1}$  and  $s_n \in [0, 1]$ . Itô expansion of the local error gives the following representation

$$\begin{aligned} \Delta e_n &= \underbrace{\int_{t_n}^{t_{n+1}} a(t, X_t^{\bar{X}_n, t_n}) - a(t_n, \bar{X}_n) dt}_{\Delta a_n} + \underbrace{\int_{t_n}^{t_{n+1}} b(t, X_t^{\bar{X}_n, t_n}) - b(t_n, \bar{X}_n) dW_t}_{\Delta b_n} \\ &= \underbrace{\int_{t_n}^{t_{n+1}} \int_{t_n}^t (a_t + a_x a + \frac{a_{xx} b^2}{2})(s, X_s^{\bar{X}_n, t_n}) ds dt}_{=:\widetilde{\Delta a_n}} + \underbrace{\int_{t_n}^{t_{n+1}} \int_{t_n}^t (a_x b)(s, X_s^{\bar{X}_n, t_n}) dW_s dt}_{=:\widetilde{\Delta a_n}} \\ &\quad + \underbrace{\int_{t_n}^{t_{n+1}} \int_{t_n}^t (b_t + b_x a + \frac{b_{xx} b^2}{2})(s, X_s^{\bar{X}_n, t_n}) ds dW_t}_{=:\widetilde{\Delta b_n}} + \underbrace{\int_{t_n}^{t_{n+1}} \int_{t_n}^t (b_x b)(s, X_s^{\bar{X}_n, t_n}) dW_s dW_t}_{=:\widetilde{\Delta b_n}}. \end{aligned} \quad (47)$$

By equation (46) we may express the MSE by the following squared sum

$$\mathbb{E} \left[ (g(X_T) - g(\bar{X}_T))^2 \right] = \mathbb{E} \left[ \left( \sum_{n=0}^{N-1} \varphi_x(\bar{X}_{n+1} + s_n \Delta e_n, t_{n+1}) \Delta e_n \right)^2 \right]. \quad (48)$$

This is the first step to deriving the error expansion in Theorem 2.1. The remaining steps follow in the proof below.

*Proof of Theorem 2.1.* The proof is derived using Taylor expansions and Itô isometry. For errors attributed to the leading order local error term  $\widetilde{\Delta b}_n$ , cf. equation (47), we will do detailed calculations, and the remainder is bounded by stated higher order terms. Let us first introduce the convenient flow map notation  $\bar{X}_n^{y, m}$  for the numerical solution at time  $t_n$  conditioned that  $\bar{X}_m = y$ , with  $m \leq n$ . Moreover, denote the first variation of the flow of the numerical solution by

$$\partial_{y_m} \bar{X}_n := \frac{\partial}{\partial y} \bar{X}_n^{y, m}, \quad m \leq n,$$

and analogously for the exact solution

$$\partial_{y_s} X_t := \frac{\partial}{\partial y} X_t^{y, s}, \quad s < t.$$

Considering the MSE error contribution from the leading order local error terms  $\widetilde{\Delta b}_n$ , i.e.,

$$\mathbb{E} \left[ \varphi_x(\bar{X}_{m+1} + s_m \Delta e_m, t_{m+1}) \varphi_x(\bar{X}_{n+1} + s_n \Delta e_n, t_{n+1}) \widetilde{\Delta b}_m \widetilde{\Delta b}_n \right], \quad (49)$$

we have for  $m = n$ ,

$$\begin{aligned} &\mathbb{E} \left[ (\varphi_x(\bar{X}_{n+1}, t_{n+1}) + \varphi_{xx}(\bar{X}_{n+1} + \hat{s}_n \Delta e_n, t_{n+1}) s_n \Delta e_n)^2 \widetilde{\Delta b}_n^2 \right] \\ &= \mathbb{E} \left[ (\varphi_x(\bar{X}_{n+1}, t_{n+1}))^2 \widetilde{\Delta b}_n^2 \right] + \mathcal{O}(\Delta t_n^3). \end{aligned} \quad (50)$$

The above  $\mathcal{O}(\Delta t_n^3)$  follows by Hölder's inequality,

$$\begin{aligned} &\mathbb{E} \left[ 2\varphi_x(\bar{X}_{n+1}, t_{n+1}) \varphi_{xx}(\bar{X}_{n+1} + \hat{s}_n \Delta e_n, t_{n+1}) s_n \Delta e_n \widetilde{\Delta b}_n^2 \right] \\ &\leq 2s_n \sqrt{\mathbb{E} \left[ (\varphi_x(\bar{X}_{n+1}, t_{n+1}) \varphi_{xx}(\bar{X}_{n+1} + \hat{s}_n \Delta e_n, t_{n+1}))^2 \right]} \sqrt{\mathbb{E} \left[ \Delta e_n^2 \widetilde{\Delta b}_n^4 \right]} \\ &\leq C \sqrt{\mathbb{E} \left[ \widetilde{\Delta b}_n^6 \right]} + o(\Delta t_n^3) = \mathcal{O}(\Delta t_n^3), \end{aligned}$$

and, by similar reasoning,

$$\mathbb{E} \left[ \varphi_{xx}(\bar{X}_{n+1} + \hat{s}_n \Delta e_n, t_{n+1})^2 s_n^2 \Delta e_n^2 \widetilde{\Delta b}_n^2 \right] = \mathcal{O}(\Delta t_n^4).$$

For achieving independence between forward paths and dual solutions in the expectations, we introduce notation for both the numerical and the exact process with the last interval Wiener increment removed:

$$\widehat{X}_{n+1} := X_{t_n} + a(X_n, t_n)\Delta t_n, \quad (51)$$

and

$$\widehat{X}_{t_{n+1}} := X_{t_n} + \int_{t_n}^{t_{n+1}} a(X_s, s)ds. \quad (52)$$

Then, a Taylor expansion leads to the equation

$$\mathbb{E}\left[\varphi_x(\overline{X}_{n+1}, t_{n+1})^2 \widetilde{\Delta b}_n^2\right] = \mathbb{E}\left[\varphi_x(\widehat{X}_{n+1}, t_{n+1})^2 \widetilde{\Delta b}_n^2\right] + o(\Delta t_n^2). \quad (53)$$

Introducing the  $\sigma$ -algebra

$$\widehat{\mathcal{F}}^n = \sigma(\{W_s\}_{0 \leq s \leq t_n}) \cup \sigma(\{W_s - W_{t_{n+1}}\}_{t_{n+1} \leq s \leq T}),$$

we observe that  $\varphi_x(\widehat{X}_{n+1}, t_{n+1})^2$  is  $\widehat{\mathcal{F}}^n$  measurable. By conditional expectation, cf. [25, App. B],

$$\begin{aligned} \mathbb{E}\left[\left(\varphi_x(\widehat{X}_{n+1}, t_{n+1})^2\right) \widetilde{\Delta b}_n^2\right] &= \mathbb{E}\left[\mathbb{E}\left[\widetilde{\Delta b}_n^2 | \widehat{\mathcal{F}}^n\right] \varphi_x(\widehat{X}_{n+1}, t_{n+1})^2\right] \\ &= \mathbb{E}\left[\varphi_x(\widehat{X}_{n+1}, t_{n+1})^2 (b_x b)^2(\overline{X}_n, t_n) \frac{\Delta t_n^2}{2}\right] + o(\Delta t_n^2), \end{aligned}$$

where the last equality used that

$$\begin{aligned} \mathbb{E}\left[\widetilde{\Delta b}_n^2 | \widehat{\mathcal{F}}^n\right] &= \mathbb{E}\left[\left(\int_{t_n}^{t_{n+1}} \int_{t_n}^t (b_x b)(s, X_s^{\overline{X}_n, t}) dW_s dW_t\right)^2 \middle| \overline{X}_n\right] \\ &= \frac{(b_x b)^2(t_n, \overline{X}_n(\omega))}{2} \Delta t_n^2 + o(\Delta t_n^2). \end{aligned}$$

Next, we show that for the terms in (49) for which  $m < n$ ,

$$\mathbb{E}\left[\varphi_x(\overline{X}_{m+1} + s_m \Delta e_m, t_{m+1}) \varphi_x(\overline{X}_{n+1} + s_n \Delta e_n, t_{n+1}) \widetilde{\Delta b}_m \widetilde{\Delta b}_n\right] = \mathcal{O}(\Delta t_n^2 \Delta t_m^2), \quad (54)$$

i.e., these terms are to the leading order negligible. To simplify computations of the expectations, we Taylor expand  $\varphi_x$  about center points that are measurable with respect to the  $\sigma$ -algebra

$$\widehat{\mathcal{F}}^{m,n} := \sigma(\{W_s\}_{0 \leq s \leq t_m}) \cup \sigma(\{W_s - W_{t_{m+1}}\}_{t_{m+1} \leq s \leq t_n}) \cup \sigma(\{W_s - W_{t_{n+1}}\}_{t_{n+1} \leq s \leq T}).$$

Our zeroth order Taylor expansion functions are  $\varphi_x\left(\widehat{X}_{n+1}^{\widehat{X}_{m+1}, t_{m+1}}, t_{n+1}\right)$  and  $\varphi_x\left(\widehat{X}_{n+1}^{\widehat{X}_{m+1}, t_{m+1}}, t_{n+1}\right)$ ,

where we recall the notation (51) and (52). Since these functions are  $\widehat{\mathcal{F}}^{m,n}$ -measurable,

$$\begin{aligned} &\mathbb{E}\left[\varphi_x(\overline{X}_{m+1} + s_m \Delta e_m, t_{m+1}) \varphi_x(\overline{X}_{n+1} + s_n \Delta e_n, t_{n+1}) \widetilde{\Delta b}_m \widetilde{\Delta b}_n\right] \\ &= \mathbb{E}\left[\mathbb{E}\left[\widetilde{\Delta b}_m \widetilde{\Delta b}_n | \widehat{\mathcal{F}}^{m,n}\right] \varphi_x\left(\widehat{X}_{n+1}^{\widehat{X}_{m+1}, t_{m+1}}, t_{n+1}\right) \varphi_x\left(\widehat{X}_{n+1}^{\widehat{X}_{m+1}, t_{m+1}}, t_{n+1}\right)\right] = 0. \end{aligned}$$

This further implies, we claim, that the leading order terms of (49) will be of the form

$$\begin{aligned} &\mathbb{E}\left\{\mathbb{E}\left[\widetilde{\Delta b}_n \left(c_{3,j} \Delta e_n + c_{4,j} \Delta W_n^2 + c_{5,j} \int_{t_n}^{t_{n+1}} b(X_s^{\widehat{X}_{m+1}, t_{m+1}}, s) dW_s\right) \times \right. \right. \\ &\quad \left. \left. \widetilde{\Delta b}_m (c_{1,j} \Delta e_m + c_{2,j} \Delta W_m^2) \middle| \widehat{\mathcal{F}}^{m,n}\right\} f_j \left(\widehat{X}_{n+1}^{\widehat{X}_{m+1}, t_{m+1}}, \widehat{X}_{n+1}^{\widehat{X}_{m+1}, t_{m+1}}, t_{n+1}\right) \right] \quad (55) \\ &= \mathcal{O}(\Delta t_m^2 \Delta t_n^2), \end{aligned}$$

for a finite number of functions  $\{f_j\}_j$  that are polynomials up to second order of  $\varphi_{xx}$ ,  $\varphi_{xxx}$ ,  $b(\bar{X}_m, t_m)$ ,  $b(\bar{X}_n, t_n)$ ,  $\partial_{y_{m+1}} \bar{X}_{n+1}^{\widehat{X}_{m+1}, t_{m+1}}$ , and up to first order of  $\partial_{y_{m+1}}^2 \bar{X}_{n+1}^{\widehat{X}_{m+1}, t_{m+1}}$ . We verify the claim (49) by identifying leading order terms of the Taylor expansions,

$$\begin{aligned}
& \varphi_x(\bar{X}_{m+1} + s_m \Delta e_m, t_{m+1}) - \varphi_x\left(\widehat{X}_{n+1}^{\widehat{X}_{m+1}, t_{m+1}}, t_{n+1}\right) \\
&= \varphi_{xx}\left(\widehat{X}_{n+1}^{\widehat{X}_{m+1}, t_{m+1}}, t_{n+1}\right) \left( s_m \Delta e_m + \check{s}_m b(\bar{X}_m, t_m) \Delta W_m + \dot{s}_n \int_{t_n}^{t_{n+1}} b(X_s^{\widehat{X}_{m+1}, t_{m+1}}, s) dW_s \right) \\
&\quad + \varphi_{xxx}\left(\widehat{X}_{n+1}^{\widehat{X}_{m+1}, t_{m+1}}, t_{n+1}\right) \left( (\check{s}_m b(\bar{X}_m, t_m) \Delta W_m)^2 + \left( \dot{s}_n \int_{t_n}^{t_{n+1}} b(X_s^{\widehat{X}_{m+1}, t_{m+1}}, s) dW_s \right)^2 \right) \\
&\quad + \text{h.o.t.}, \tag{56}
\end{aligned}$$

and

$$\begin{aligned}
& \varphi_x(\bar{X}_{n+1} + s_n \Delta e_n, t_{n+1}) - \varphi_x\left(\widehat{X}_{n+1}^{\widehat{X}_{m+1}, t_{m+1}}, t_{n+1}\right) \\
&= \varphi_{xx}\left(\widehat{X}_{n+1}^{\widehat{X}_{m+1}, t_{m+1}}, t_{n+1}\right) \left( s_n \Delta e_n + \dot{s}_n b(\bar{X}_n^{\widehat{X}_{m+1}, t_{m+1}}, t_n) \Delta W_n \right. \\
&\quad \left. + \partial_{y_{m+1}} \bar{X}_{n+1}^{\widehat{X}_{m+1}, t_{m+1}} \check{s}_m b(\bar{X}_m, t_m) \Delta W_m + \partial_{y_{m+1}}^2 \bar{X}_{n+1}^{\widehat{X}_{m+1}, t_{m+1}} (\check{s}_m b(\bar{X}_m, t_m) \Delta W_m)^2 \right) \tag{57} \\
&\quad + \varphi_{xxx}\left(\widehat{X}_{n+1}^{\widehat{X}_{m+1}, t_{m+1}}, t_{n+1}\right) \left( \left( \dot{s}_n b(\bar{X}_n^{\widehat{X}_{m+1}, t_{m+1}}, t_n) \Delta W_n \right)^2 \right. \\
&\quad \left. + \left( \partial_{y_{m+1}} \bar{X}_{n+1}^{\widehat{X}_{m+1}, t_{m+1}} \check{s}_m b(\bar{X}_m, t_m) \Delta W_m \right)^2 \right) + \text{h.o.t.}
\end{aligned}$$

Equation (55) then follows by Itô isometry.

So far we have shown that

$$\begin{aligned}
& \mathbb{E} \left[ \left( \sum_{n=0}^{N-1} \varphi_x(\bar{X}_{n+1} + s_n \Delta e_n, t_{n+1}) \widetilde{\Delta b}_n \right)^2 \right] \\
&= \mathbb{E} \left[ \sum_{n=0}^{N-1} \varphi_x\left(\widehat{X}_{n+1}, t_{n+1}\right)^2 \frac{(b_x b)^2}{2} (\bar{X}_n, t_n) \Delta t_n^2 + o(\Delta t_n^2) \right] \tag{58} \\
&= \mathbb{E} \left[ \sum_{n=0}^{N-1} \varphi_x(\bar{X}_{n+1}, t_{n+1})^2 \frac{(b_x b)^2}{2} (\bar{X}_n, t_n) \Delta t_n^2 + o(\Delta t_n^2) \right].
\end{aligned}$$

The MSE contribution from the other local error terms  $\widetilde{\Delta a}_n$ ,  $\widetilde{\Delta a}_n$  and  $\widetilde{\Delta b}_n$  can also be bounded using the above approach with Taylor expansions,  $\widehat{\mathcal{F}}^{m,n}$ -conditioning and Itô isometries, yielding

$$\begin{aligned}
& \mathbb{E} \left[ \varphi_x(\bar{X}_{m+1} + s_m \Delta e_m, t_{m+1}) \varphi_x(\bar{X}_{n+1} + s_n \Delta e_n, t_{n+1}) \widetilde{\Delta a}_m \widetilde{\Delta a}_n \right] \\
&= \mathbb{E} \left[ \varphi_x(\bar{X}_{m+1}, t_{m+1}) \varphi_x(\bar{X}_{n+1}, t_{n+1}) \left( \frac{a_t + a_x a + a_{xx} b^2 / 2}{2} \right) (\bar{X}_m, t_m) \times \right. \\
&\quad \left. \left( \frac{a_t + a_x a + a_{xx} b^2 / 2}{2} \right) (\bar{X}_n, t_n) \Delta t_m^2 \Delta t_n^2 \right] + o(\Delta t_m^2 \Delta t_n^2), \tag{59}
\end{aligned}$$

$$\begin{aligned} & \mathbb{E} \left[ \varphi_x(\bar{X}_{m+1} + s_m \Delta e_m, t_{m+1}) \varphi_x(\bar{X}_{n+1} + s_n \Delta e_n, t_{n+1}) \widetilde{\Delta a}_m \widetilde{\Delta a}_n \right] \\ &= \begin{cases} \mathbb{E} \left[ \varphi_x(\bar{X}_{n+1}, t_{n+1})^2 \frac{(a_x b)^2}{2} (\bar{X}_n, t_n) \Delta t_n^3 + o(\Delta t_n^3) \right], & \text{if } m = n, \\ \mathcal{O}(\Delta t_m^2 \Delta t_n^2), & \text{if } m \neq n, \end{cases} \end{aligned} \quad (60)$$

and

$$\begin{aligned} & \mathbb{E} \left[ \varphi_x(\bar{X}_{m+1} + s_m \Delta e_m, t_{m+1}) \varphi_x(\bar{X}_{n+1} + s_n \Delta e_n, t_{n+1}) \widetilde{\Delta b}_m \widetilde{\Delta b}_n \right] \\ &= \begin{cases} \mathbb{E} \left[ \varphi_x(\bar{X}_{n+1}, t_{n+1})^2 \frac{(b_t + b_x a + b_x b^2/2)^2}{3} (\bar{X}_n, t_n) \Delta t_n^3 + o(\Delta t_n^3) \right], & \text{if } m = n, \\ \mathcal{O}(\Delta t_m^2 \Delta t_n^2), & \text{if } m \neq n. \end{cases} \end{aligned} \quad (61)$$

Moreover, MSE error contributions involving products of different local error terms, e.g.,  $\widetilde{\Delta a}_m \widetilde{\Delta b}_n$ , are also bounded in the same fashion, giving  $\mathcal{O}(\Delta t_n^3)$  when  $m = n$  and  $\mathcal{O}(\Delta t_m^2 \Delta t_n^2)$  when  $m \neq n$ .

The proof is completed by two replacement steps. First, replacing the first variation of the exact path  $\varphi_x(\bar{X}_{n+1}, t_{n+1})$  in (58) with the first variation of the numerical solution  $\bar{\varphi}_{x,n+1} := \frac{\partial}{\partial \bar{X}_{n+1}} g(\bar{X}_T)$ . Under sufficient regularity, this replacement possible without introducing additional leading order error terms as it is shown in [29, p. 29] that

$$\mathbb{E} [ |\bar{\varphi}_{x,n+1} - \varphi_x(\bar{X}_{n+1}, t_{n+1})| ] = \mathcal{O} \left( \max_n \sqrt{\Delta t_n} \right). \quad (62)$$

And second, replacing  $\bar{\varphi}_{x,n+1}$  by  $\bar{\varphi}_{x,n}$ , which also is possible under sufficient regularity, since equation (14) implies that

$$\mathbb{E} [ |\bar{\varphi}_{x,n} - \bar{\varphi}_{x,n+1}| ] = \mathcal{O} \left( \sqrt{\Delta t_n} \right).$$

□

**A.2. Error expansion for the MSE in multi-dimensions.** In this section, we extend the 1D MSE error expansion presented in Theorem 2.1 to the multi-dimensional setting.

Considering the SDE

$$\begin{aligned} dX_t &= a(X_t, t) dt + b(X_t, t) dW_t, \\ X_0 &= x_0, \end{aligned} \quad (63)$$

where  $X : [0, T] \rightarrow \mathbb{R}^d$ ,  $W : [0, T] \rightarrow \mathbb{R}^m$ ,  $a : \mathbb{R}^d \times [0, T] \rightarrow \mathbb{R}^d$  and  $b : \mathbb{R}^d \times [0, T] \rightarrow \mathbb{R}^{d \times m}$ . Let further  $x_i$  denote  $i$ -th element of an arbitrary vector  $x$ , and  $b^{(i,j)}$  and  $b^T$  denote respectively the  $(i, j)$ -th element and the transpose of the diffusion matrix  $b$ . (To avoid confusion, this derivation does not make use of any MLMC notation, particularly not the multilevel superscript  $\cdot^{\{\ell\}}$ .)

Using the Einstein summation convention to sum over spatial/dimensional indices, but not over the time index  $n$ , the 1D local error terms in equation (47) generalize into

$$\begin{aligned} \widetilde{\Delta a}_n^{(i)} &= \int_{t_n}^{t_{n+1}} \int_{t_n}^t \left( a_t^{(i)} + a_{x_j}^{(i)} a^{(j)} + \frac{1}{2} a_{x_j x_k}^{(i)} (bb^T)^{(j,k)} \right) ds dt, \\ \widetilde{\Delta a}_n^{(i)} &= \int_{t_n}^{t_{n+1}} \int_{t_n}^t a_{x_j}^{(i)} b^{(j,k)} dW_s^{(k)} dt, \\ \widetilde{\Delta b}_n^{(i)} &= \int_{t_n}^{t_{n+1}} \int_{t_n}^t b_t^{(i,j)} + b_{x_k}^{(i,j)} a^{(k)} + \frac{1}{2} b_{x_k x_\ell}^{(i,j)} (bb^T)^{(k,\ell)} ds dW_t^{(j)}, \\ \widetilde{\Delta b}_n^{(i)} &= \int_{t_n}^{t_{n+1}} \int_{t_n}^t b_{x_k}^{(i,j)} b^{(k,\ell)} dW_s^{(\ell)} dW_t^{(j)}, \end{aligned}$$

where all the above integrand functions in all equations implicitly depend on the state argument  $X_s^{\bar{X}_n, t_n}$ , in flow notation, e.g.,  $a_t^{(i)}$  is shorthand for  $a_{x_j}^{(i)}(X_s^{\bar{X}_n, t_n}, s)$ .

Under sufficient regularity, a tedious calculation similar to the proof of Theorem 2.1 verifies that for a given smooth payoff  $g : \mathbb{R}^d \rightarrow \mathbb{R}$ ,

$$\mathbb{E} \left[ (g(X_T) - g(\bar{X}_T))^2 \right] \leq \mathbb{E} \left[ \sum_{n=0}^{N-1} \bar{\rho}_n \Delta t_n^2 + o(\Delta t_n^2) \right], \quad (64)$$

where

$$\bar{\rho} := \frac{1}{2} \bar{\varphi}_{x_i, n} \left( (bb^T)^{(k, \ell)} (b_{x_k} b_{x_\ell}^T) \right)^{(i, j)} (\bar{X}_n, t_n) \bar{\varphi}_{x_j, n}. \quad (65)$$

In the multi-dimensional setting, one may show that  $\varphi_x(y, t) = \partial_y g(X_T^{y, t}) \in \mathbb{R}^d$  formally solves

$$\begin{aligned} -d\varphi_x(X_s^{y, t}, s) &= (a_x(X_s^{y, t}, s)ds + b_x(X_s^{y, t}, s)dW_s)^T \varphi_x(X_s^{y, t}, s), \quad t < s < T, \\ \varphi_x(X_T^{y, t}, T) &= g'(X_T^{y, t}), \end{aligned} \quad (66)$$

cf. [29]. The corresponding extension of the numerical method (14) reads

$$\begin{aligned} \bar{\varphi}_{x, n} &= C_x^T(\bar{X}_n, t_n) \bar{\varphi}_{x, n+1}, \quad n = N-1, N-2, \dots, 0. \\ \bar{\varphi}_{x, N} &= g'(\bar{X}_T), \end{aligned} \quad (67)$$

with  $C : \mathbb{R}^d \times [0, T] \rightarrow \mathbb{R}^d$  defined by

$$C(\bar{X}_n, t_n) = \bar{X}_n + a(\bar{X}_n, t_n)\Delta t_n + b(\bar{X}_n, t_n)\Delta W_n.$$

#### APPENDIX B. A UNIFORM TIME STEP MLMC ALGORITHM

The uniform time step MLMC method for MSE approximations of SDE was proposed in [8]. Below, we present the version of that method that we use in the numerical tests in this paper for reaching the approximation goal (2).

---

#### Algorithm 5 mlmcEstimator

---

**Input:**  $\text{TOL}_T$ ,  $\text{TOL}_S$ , confidence  $\delta$ , input mesh  $\Delta t^{\{-1\}}$ , input mesh intervals  $N_{-1}$ , initial number of samples  $\widehat{M}$ , weak convergence rate  $\alpha$ , SDE problem.

**Output:** Multilevel estimator  $\mathcal{A}_{\mathcal{MLC}}$ .

Compute the confidence parameter  $C_C(\delta)$  by (37).

Set  $L = -1$ .

**while**  $L < 3$  **or** (39), using the input rate  $\alpha$ , is violated **do**

  Set  $L = L + 1$ .

  Set  $M_L = \widehat{M}$ , generate a set of (Euler–Maruyama) realizations  $\{\Delta_\ell g(\omega_{i, \ell})\}_{i=1}^{M_L}$  on mesh and Wiener path pairs  $(\Delta t^{\{L-1\}}, \Delta t^{\{L\}})$  and  $(W^{\{L-1\}}, W^{\{L\}})$ , where the uniform mesh pairs have step sizes  $\Delta t^{\{L-1\}} = T/N_{L-1}$  and  $\Delta t^{\{L\}} = T/N_L$ , respectively.

**for**  $\ell = 0$  **to**  $L$  **do**

    Compute the sample variance  $\mathcal{V}(\Delta_\ell g; M_\ell)$ .

**end for**

**for**  $\ell = 0$  **to**  $L$  **do**

    Determine the number of samples by

$$M_\ell = \left\lceil \frac{C_C^2}{\text{TOL}_S^2} \sqrt{\frac{\text{Var}(\Delta_\ell g)}{N_\ell}} \sum_{\ell=0}^L \sqrt{N_\ell \text{Var}(\Delta_\ell g)} \right\rceil.$$

    (The equation for  $M_\ell$  is derived by Lagrangian optimization, cf. Section 3.2.1.)

**if** New value of  $M_\ell$  is larger than the old value **then**

      Compute additional (Euler–Maruyama) realizations  $\{\Delta_\ell g(\omega_{i, \ell})\}_{i=M_\ell+1}^{M_\ell^{new}}$  on mesh and Wiener path pairs  $(\Delta t^{\{\ell-1\}}, \Delta t^{\{\ell\}})$  and  $(W^{\{\ell-1\}}, W^{\{\ell\}})$ , where the uniform mesh pairs have step sizes  $\Delta t^{\{\ell-1\}} = T/(2^\ell N_{-1})$  and  $\Delta t^{\{\ell\}} = T/(2^{\ell+1} N_{-1})$ , respectively.

**end if**

**end for**

**end while**

Compute  $\mathcal{A}_{\mathcal{MLC}}$  using the generated samples by the formula (7).

---

**Acknowledgments.** The authors would like to thank Arturo Kohatsu-Higa for his helpful suggestions for improvements in the proof of Theorem 2.1.

**Support** This work was supported by King Abdullah University of Science and Technology (KAUST), the University of Austin Subcontract (Project Number 024550, Center for Predictive Computational Science), and the VR project ”Effektiva numeriska metoder för stokastiska differentialekvationer med tillämpningar”. The first author was and the third author is a member of the Research Center on Uncertainty Quantification in Computational Science and Engineering at KAUST.

## REFERENCES

- [1] R. Avikainen. On irregular functionals of SDEs and the Euler scheme. *Finance and Stochastics*, 13(3):381–401, 2009.
- [2] W. Bangerth and R. Rannacher. *Adaptive finite element methods for differential equations*. Lectures in Mathematics ETH Zürich. Birkhäuser Verlag, Basel, 2003.
- [3] A. Barth and A. Lang. Multilevel Monte Carlo method with applications to stochastic partial differential equations. *Int. J. Comput. Math.*, 89(18):2479–2498, 2012.
- [4] K. A. Cliffe, M. B. Giles, R. Scheichl, and A. L. Teckentrup. Multilevel Monte Carlo methods and applications to elliptic PDEs with random coefficients. *Comput. Vis. Sci.*, 14(1):3–15, 2011.
- [5] N. Collier, A.-L. Haji-Ali, F. Nobile, E. von Schwerin, and R. Tempone. A Continuation Multilevel Monte Carlo algorithm. *ArXiv e-prints*, February 2014.
- [6] R. Durrett. *Probability: theory and examples*. Duxbury Press, Belmont, CA, second edition, 1996.
- [7] J. G. Gaines and T. J. Lyons. Variable step size control in the numerical solution of stochastic differential equations. *SIAM J. Appl. Math.*, 57:1455–1484, 1997.
- [8] M. B. Giles. Multilevel Monte Carlo path simulation. *Oper. Res.*, 56(3):607–617, 2008.
- [9] M. B. Giles and L. Szpruch. Antithetic multilevel Monte Carlo estimation for multi-dimensional SDEs without Lévy area simulation. *Ann. Appl. Probab.*, 24(4):1585–1620, 2014.
- [10] D. T. Gillespie. The chemical Langevin equation. *The Journal of Chemical Physics*, 113(1):297–306, 2000.
- [11] P. Glasserman. *Monte Carlo methods in financial engineering*, volume 53 of *Applications of Mathematics (New York)*. Springer-Verlag, New York, 2004. Stochastic Modelling and Applied Probability.
- [12] S. Heinrich. Monte Carlo complexity of global solution of integral equations. *J. Complexity*, 14(2):151–175, 1998.
- [13] S. Heinrich and E. Sindambiwe. Monte Carlo complexity of parametric integration. *J. Complexity*, 15(3):317–341, 1999.
- [14] H. Hoel, E. von Schwerin, A. Szepessy, and R. Tempone. Implementation and analysis of an adaptive multilevel Monte Carlo algorithm. *Monte Carlo Methods and Applications*, 20(1):1–41, 2014.
- [15] N. Hofmann, T. Müller-Gronbach, and K. Ritter. Optimal approximation of stochastic differential equations by adaptive step-size control. *Math. Comp.*, 69(231):1017–1034, 2000.
- [16] J. D. Hunter. Matplotlib: A 2d graphics environment. *Computing in Science Engineering*, 9(3):90–95, may-june 2007.
- [17] S. Ilie. Variable time-stepping in the pathwise numerical solution of the chemical Langevin equation. *The Journal of Chemical Physics*, 137(23):–, 2012.
- [18] A. Kebaier. Statistical Romberg extrapolation: A new variance reduction method and applications to option pricing. *Ann. Appl. Probab.*, 15(4):2681–2705, 2005.
- [19] P. E. Kloeden and E. Platen. *Numerical solution of stochastic differential equations*, volume 23 of *Applications of Mathematics (New York)*. Springer-Verlag, Berlin, 1992.
- [20] H. Lamba, J. C. Mattingly, and A. M. Stuart. An adaptive Euler-Maruyama scheme for SDEs: convergence and stability. *IMA J. Numer. Anal.*, 27(3):479–506, 2007.
- [21] A. Lateef Haji-Ali, F. Nobile, E. von Schwerin, and R. Tempone. Optimization of mesh hierarchies in Multilevel Monte Carlo samplers. *ArXiv e-prints*, March 2014.
- [22] P. L’Ecuyer and E. Buist. Simulation in Java with SSJ. In *Proceedings of the 37th conference on Winter simulation*, WSC ’05, pages 611–620. Winter Simulation Conference, 2005.
- [23] G. N. Milstein and M. V. Tretyakov. Quasi-symplectic methods for Langevin-type equations. *IMA J. Numer. Anal.*, 23(4):593–626, 2003.
- [24] S. Mishra and C. Schwab. Sparse tensor multi-level Monte Carlo finite volume methods for hyperbolic conservation laws with random initial data. *Math. Comp.*, 81(280):1979–2018, 2012.
- [25] B. Øksendal. *Stochastic differential equations*. Universitext. Springer-Verlag, Berlin, fifth edition, 1998.
- [26] E. Platen and D. Heath. *A benchmark approach to quantitative finance*. Springer Finance. Springer-Verlag, Berlin, 2006.
- [27] S. E. Shreve. *Stochastic calculus for finance. II*. Springer Finance. Springer-Verlag, New York, 2004. Continuous-time models.
- [28] R. D. Skeel and J. A. Izaguirre. An impulse integrator for Langevin dynamics. *Molecular Physics*, 100(24):3885–3891, 2002.

- [29] A. Szepessy, R. Tempone, and G. E. Zouraris. Adaptive weak approximation of stochastic differential equations. *Comm. Pure Appl. Math.*, 54(10):1169–1214, 2001.
- [30] D. Talay. Stochastic Hamiltonian systems: exponential convergence to the invariant measure, and discretization by the implicit Euler scheme. *Markov Process. Related Fields*, 8(2):163–198, 2002. Inhomogeneous random systems (Cergy-Pontoise, 2001).
- [31] D. Talay and L. Tubaro. Expansion of the global error for numerical schemes solving stochastic differential equations. *Stochastic Analysis and Applications*, 8(4):483–509, 1990.
- [32] A. L. Teckentrup, R. Scheichl, M. B. Giles, and E. Ullmann. Further analysis of multilevel Monte Carlo methods for elliptic PDEs with random coefficients. *Numer. Math.*, 125(3):569–600, 2013.
- [33] L. Yan. The Euler scheme with irregular coefficients. *The Annals of Probability*, 30(3):1172–1194, 2002.